Nithin Kumar[1], Prabhakaran Ramya Bala[1], Diptimayee Behera[2], Ambili Anoop[2], and Raman Sukumar[3]

[1]National Institute of Advanced Studies
[2]Indian Institute of Science Education and Research
[3]Indian Institute of Science

July 13, 2023

Abstract

A major fire raged through the dry tropical forests of Bandipur Tiger Reserve, a 'biodiversity hotspot' in southern India, in February 2019. The fire occurred in patches, burning >10,000 acres of forest, becoming one of the largest forest fires in India in recent times. Very few studies have been able to capture the dynamics of fire proxies from an active surface fire, especially in the dry tropics. We opportunistically sampled two wetlands roughly sandwiched between the largest and the second-largest burnt patches a week after the fire was extinguished. We collected surface samples from each wetland and looked at popular fire proxies – macrocharcoal, microcharcoal, microcharcoal/pollen (C/P) ratio and the abundance and distribution of Polycyclic Aromatic Hydrocarbons (PAHs). Macrocharcoal counts were low (mean ˜5), while the C/P ratio was ˜1. Low Molecular Weight (LMW) PAH molecules Phenanthrene, Anthracene, Fluoranthene and Pyrene were found in both sites, while High Molecular Weight (HMW) PAHs were only found in one. None of the proxies is particularly indicative of the large surface fire that occurred ˜15 km away. Analysis of wind speed and direction from weather station data and forward and backward HYSPLIT model trajectories tell us that both wetlands were not downstream of the smoke plume. There was also no recorded precipitation between the fire event and the sampling date. Through this opportunistic study of fire proxies, we show that wind direction and wet scavenging are essential factors determining the transport and deposition of fire proxies in this environment. Hence reconstruction of fire histories should be done using multi-site data since the absence of fire proxies does not equate to the absence of fire.

Surface sampling of wetlands in a tropical dry forest after a large fire: Wind direction dominates the transport and deposition of fire proxies

Nithin Kumar[1], Prabhakaran Ramya Bala[1]*, Diptimayee Behera[2], Ambili Anoop[2], Raman Sukumar[3]

[1]National Institute of Advanced Studies, Bangalore, India
[2]Indian Institute of Science Education and Research, Mohali,India
[3]Indian Institute of Science, Bangalore,India

* Corresponding author - Prabhakaran Ramya Bala – pramyabala@gmail.com, pramyabala@nias.res.in

Abstract

A major fire raged through the dry tropical forests of Bandipur Tiger Reserve, a ‘biodiversity hotspot’ in southern India, in February 2019. The fire occurred in patches, burning >10,000 acres of forest, becoming one of the largest forest fires in India in recent times. Very few studies have been able to capture the dynamics of fire proxies from an active surface fire, especially in the dry tropics. We opportunistically sampled two wetlands roughly sandwiched between the largest and the second-largest burnt patches a week after the fire was extinguished. We collected surface samples from each wetland and looked at popular fire proxies – macrocharcoal, microcharcoal, microcharcoal/pollen (C/P) ratio and the abundance and distribution of Polycyclic Aromatic Hydrocarbons (PAHs). Macrocharcoal counts were low (mean ~5), while the C/P ratio was ~1. Low Molecular Weight (LMW) PAH molecules Phenanthrene, Anthracene, Fluoranthene and Pyrene were found in both sites, while High Molecular Weight (HMW) PAHs were only found in one. None of the proxies is particularly indicative of the large surface fire that occurred ~15 km away. Analysis of wind speed and direction from weather station data and forward and backward HYSPLIT model trajectories tell us that both wetlands were not downstream of the smoke plume. There was also no recorded precipitation between the fire event and the sampling date. Through this opportunistic study of fire proxies, we show that wind direction and wet scavenging are essential factors determining the transport and deposition of fire proxies in this environment. Hence reconstruction of fire histories should be done using multi-site data since the absence of fire proxies does not equate to the absence of fire.

Introduction

Approximately 420 million years ago (late Silurian Period) the emergence of land vascular plants (Beerling, 2007) and the rise in the photosynthetic atmospheric oxygen (>13%), made fire ignition possible on Earth (Bowman et al., 2009; Glasspool et al., 2004; Scott, 2000a; Scott and Glasspool, 2006). By Late Tertiary, increase in oxygen (Berner, 2006) and burnable biomass, fire became a global phenomenon capable of changing and shaping every terrestrial ecosystem across the globe (Herring, 2013; Jia et al., 2003; Pausas and Keeley, 2009). In addition to being a global terrestrial modifier, fire also played a critical role in human evolution as well. Cooking meat aided in the development of brain size, bipedalism, and utilization of stone tools (Dunbar, 2009). The knowledge of ignition and management of fire came out much later, out of necessity, due to the temperature drop from the warm Pliocene to Pleistocene ice ages (deMenocal, 2004; Glikson, 2013). From 790-690 kyr, humans started using fire more extensively (deMenocal, 2004) and subsequently, they started to make appreciable effects on the forest ecology (Archibald et al., 2012; Bowman et al., 2011; D. Burton, 2009; Marlon et al., 2009). With these increased anthropogenic pressures and the changes induced due to climate change and global warming on fire-prone ecosystems, several concerns have been raised about their fate and resilience (Bowman, 2015; Flannigan et al., 2009; Foley et al., 2013; Lawson et al., 2013; Schumacher and Bugmann, 2006). The information that is required to answer such concerns is achieved through the study of the long-term trends of vegetation and fire histories.

In the last 50 years, several palaeoecological investigation techniques have been developed to aid this process. This includes the investigation through charcoal particles (Clark, 1988; Leys et al., 2013; Scott, 2000b; Tinner and Hu, 2003; Vachula, 2021; Whitlock and Larsen, 2002) Polycyclic Aromatic Hydrocarbons (PAHs) (Denis et al., 2012; Edwards, 1983; Kong et al., 2021; Musa Bandowe et al., 2014; Vachula et al., 2022; Yunker et al., 2002) in archeological material and natural paleoenvironmental archives, magnetic susceptibility of soil (Gedye et al., 2000; Rummery, 1983), fire scars in dendrochronology (Stephens et al., 2003), and also from historical documents. Of all these methods, charcoal-based reconstruction is the most widely used due to several advantages. Charcoal is inert (Scott, 2010), which results in its being well-preserved in a wide variety of environmental conditions. Charcoal has the potential to predict various characteristics of fire like

intensity (Duffin et al., 2008), severity (Whitlock and Larsen, 2002), extent, and frequency (Leys et al., 2013). Charcoal morphologies have also been used to trace the type of vegetation burnt (Enache and Cumming, 2006; Frank-DePue et al., 2022; Jensen et al., 2007; Mustaphi and Pisaric, 2014). The latter has developed an elaborate classification of sedimentary charcoal particles to identify fuel sources. Particles were categorized into seven major morphological classes (A to G) based on the overall shape, subdivided into 27 subclasses based on dominant surface textures or major features. With this classification scheme, they introduced an identification flow chart to identify fuel sources. Charcoal has also been combined with other proxies such as pollen (MacDonald et al., 1991), phytolith (Gu et al., 2007), molecular fire proxies (Argiriadis et al., 2018; Conedera et al., 2009; Denis et al., 2012; Musa Bandowe et al., 2014; Vachula et al., 2022) waxes (Lerch et al., 2022) and, sterols (Argiriadis et al., 2018). Since several other proxies can be simultaneously analyzed and creatively combined with charcoal, it provides robust ways of examining linkages between forest fires, vegetation, and anthropogenic activities.

However, these reconstruction techniques with charcoal are not without problems. The lack of standardization in extraction procedures, identification, and quantification of macrocharcoal (Conedera et al., 2009) is of great concern. The uncertainties in relationships between particle size, burnt area, and dispersal distance (Clark, 1988; Higuera et al., 2007; Marlon et al., 2009; Vachula, 2021; Vachula et al., 2018; Vachula and Richter, 2018) as well as the use of charcoal morphology to trace fuel sources are yet to be resolved (Enache and Cumming, 2006; Frank-DePue et al., 2022; Mustaphi and Pisaric, 2014). There are also variability associated with the production rate of charcoal depending on the vegetation burned (Feurdean, 2021; Pereboom et al., 2020; Vachula et al., 2022). Additionally, factors like wind speed and direction, morphology and size of the airborne particles, geographic location of sampling and source sites are also likely to affect the distribution, deposition, and retrieval of these proxies.

Another recently developing fire indicator is the polycyclic aromatic hydrocarbons (PAHs). They are produced either by the combustion of fossil fuels or by the burning of organic materials during a forest fire (Edwards, 1983). The source of the PAH can be distinguished by certain ratios of specific PAHs (Denis et al., 2012; Vachula et al., 2022; Yunker et al., 2002). There are several advantages associated with this proxy. The PAH produced can vary depending on the combustion temperature

(Blumer, 1976; Laflamme and Hites, 1978) and they have a broader temperature range than charcoal (Conedera et al., 2009; Lu et al., 2009). Moreover, PAH assemblages also vary with fuel type, fuel moisture and oxygen availability (Burns et al., 1997; Lu et al., 2009; Yang et al., 2007). Thus, PAH analysis can give a lot of information about the fire event and the fuel sources, similar to charcoal. A few studies have in fact used PAH as indicators of fire along with charcoal (Denis et al., 2012; Kong et al., 2021; Vachula et al., 2022; Yunker et al., 2002) but there are problems associated with this as well. The significant ones being lack of understanding of the factors that control their production, spatial distribution, and deposition mechanism. The PAH in the sediment can also undergo microbial degradation, especially the low molecular ones, leading to its depletion in the sediment (Yan et al., 2022, 2021). Further, the low molecular ones are also subjected to degradation during transport (Vachula et al., 2022).

Thus, certain aspects of these proxies (charcoal and PAH) are not very well understood and thus require a modern fire-proxy calibration to see how these proxies are captured and preserved in environmental archives. It also gives an idea on how they behave during after the fire event and also about the transport mechanism. Studies have been conducted on various fire-prone ecosystems like temperate, boreal, subalpine forests, grasslands, and savannahs across the world, making use of atmospheric and lake sediment traps, lake sediment cores, and lake surface sampling (Aleman et al., 2013; Clark et al., 1998; Leys et al., 2015; Lynch et al., 2004; Pisaric, 2002; Tinner et al., 2006). But none have been reported so far from the frequently burning tropical dry forests, especially from India, and this would be the first study reporting it.

In this study, we look at the modern fire-proxy relationship in the dry tropical forests of southern India, through an opportunistic sampling of two wetlands in the Mudumalai Tiger Reserve (MTR), after a fire broke out on 22 February 2019. The fire occurred in patches, in the forests of Bandipur, Wayanad, and Mudumalai Tiger reserves of the Nilgiris Biosphere Reserve in the Western Ghats. According to a newspaper report, this was purported to be a man-made disaster caused by miscreants deliberately setting elephant dung on fire (Chennabasaveshwar, 2019) . The initial fires were brought under control within hours, but the dominant easterly winds of > 9km/hr speed (Kargudi weather station data), aided its spread, burning an area of more than10,920 acres in just three days. The fire was brought under control by 26 February by the collective effort of forest officials, local

people, volunteers from the public and the Indian Air Force. A satellite study reported that the land temperature during the fire reached up to 140^0C (Iyer et al., 2021). Even a week after the main fire event, complete extinguishment of the residual fire was not achieved.

Methods

Sample location

The samples were collected from two wetlands, Ombetta (110 34’36.73″’N, 76036’29.24’’E) and Imbrella (11034’36.73’’N, 76031’29.24’’E), one week after the fire, on 7 March 2019 (Fig 1). The fire occurred in patches with the largest area burnt in the Bandipur Tiger reserve (BTR), while a second, smaller patch burnt in the adjacent Mudumalai Tiger reserve (MTR). Ombetta is ~5 km north of the MTR patch and 15 km south of the BTR patch. Imbrella is located ~7 km north of the MTR patch and 10 km south of the BTR fire patch. These two wetlands are separated by a distance of about three kilometers.

Sample Collection

A total of 20 samples, 10 from each wetland were collected by walking along the edges. The ten samples comprise of five surface samples collected by scooping 2 cm of the surface and five bottle core samples collected by pressing a 5 cm tall plastic bottle into the sediment and collecting the contents. The collected samples were stored in a freezer in the field base at -20° C. They were transported in frozen state to the lab at the Indian Institute of Science, Bengaluru, where they were freeze-dried (Labconco bulk drier), crushed gently using pestle and mortar and stored in room temperature until further analysis.

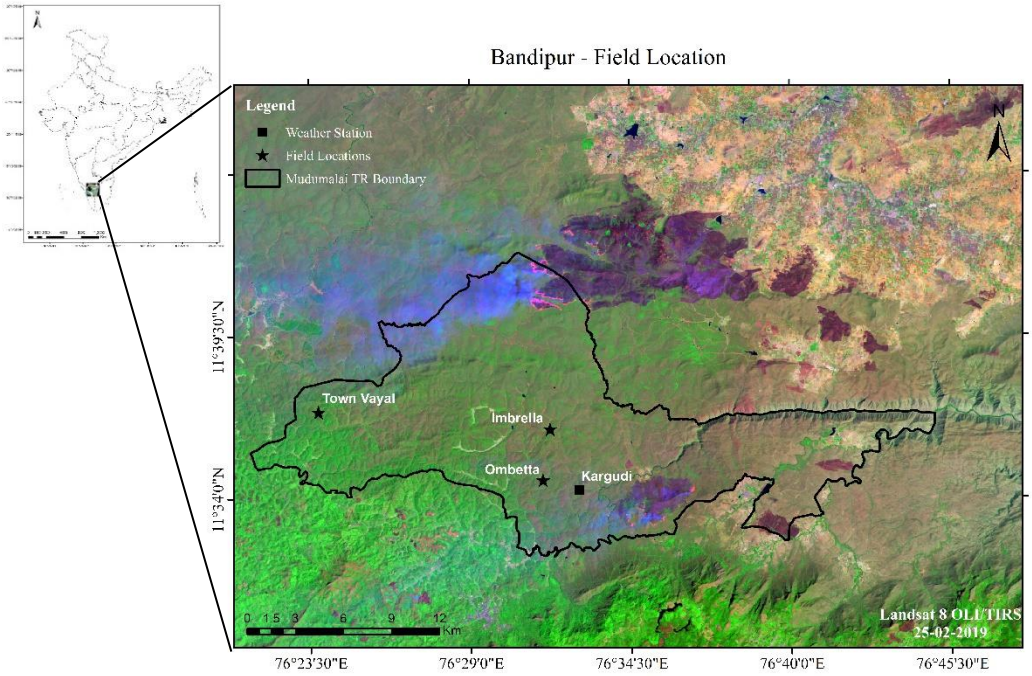

Fig 1: Landsat Image of Mudumalai Tiger Reserve (MTR) during the final day of the fire. The black line demarcates MTR boundaries. Imbrella and Ombetta (black stars) are the sampling wetlands, black square is the Kargudi weather station from which the wind data was collected. Two dark violet patches on the top of MTR and southeast of Kargudi are the major fire patches. The fire started in east and spread towards the west. You can see smoke arising moving west.

Macrocharcoal analysis

One gram of sample was taken and kept in 10ml of 10% sodium hexametaphosphate $(NaPO_3)_6$) solution overnight to deflocculate the sediments. We found Sodium hexametaphosphate was better in dispersing the clay than KOH (Andreola et al., 2004). This was followed by Sodium hypochlorite (NaOCl) treatment to bleach the organics (Stevenson and Haberle, 2005). The samples were then sieved through a 125 µm mesh and residue >125 µm was collected for identification. Macrocharcoal particles are black, opaque and usually planar and were counted under a stereomicroscope (LeicaS4E) at 10X magnification. For each sample, three extractions were done and the charcoal particles counted, its mean, median, maximum and minimum values are given in fig 2.

Microcharcoal and Pollen counts

Microcharcoal extraction was done using the same method used for pollen (Bennett, 1990), the standard procedure followed at the French Institute of Pondicherry (FIP). In this method, samples are treated with a dispersing agent and coarse particles (>150 µm) and clay particles are removed. Then it is treated with 10% hydrochloric acid (HCl) to remove carbonates and (48%) hydrofluoric Acid (HF) to remove silicates. This is followed by acetolysis (9:1 mixture of acetic anhydride $(CH_3CO)_2O$ and sulfuric acid (H_2SO_4) to remove polysaccharides (Gunnar, 1960).The sample is then centrifuged and the supernatant is removed. The extracts were mounted on glass slides using glycerin. Both microcharcoal and pollen grains were counted (minimum of 1000 pollen) under a microscope (Olympus CX43). Pollen counting was done using the Thanikaimoni reference collection at (FIP) (Anupama et al., 2014;).

Polycyclic Aromatic Hydrocarbons (PAHs)

Sediment samples, in powdered form (~6 g), were combined homogeneously with unsaturated silica. This blend was subsequently packed into stainless steel enclosures and subjected to lipid extraction in a Buchi Speed Extractor E-914. The solvent mixture used was dichloromethane (DCM) and methanol in a ratio of 93:7. The extractor parameters were set to conduct two cycles at a temperature of 100 °C and a pressure of 70 bar, facilitating the maximal extraction of organic material. Post extraction, the substance obtained was concentrated carefully at 30 °C using a Buchi P-6 Multivapor. The total lipid extract (TLE) dissolved in 2 ml of hexane, was then transferred into a glass column filled with 2 cm of glass wool and 17 cm of silica gel. 20 ml of hexane was used to isolate the saturated hydrocarbon component from the TLE. The aromatic fraction was eluted using 80 ml of a solution of hexane-DCM in the ratio of 4:1. This fraction was then completely condensed via dry nitrogen gas and dissolved in a final volume of 0.5 ml DCM for further analysis (Ajay et al., 2021; Behera et al., 2022)

The fractionated aliquots were subjected to analytical testing using gas chromatography-mass spectrometry (GC-MS; Agilent 7890B/5977 MSD), adhering to the procedure detailed in (Behera et al., 2022). A non-polar capillary column (HP5-MS, with dimensions of 30 m × 250 µm × 0.25

μm) was utilized for this analysis, with helium as carrier gas. The injection method used was spitless, with the inlet temperature set at 320 °C and a maximum sample volume of 1 μL. The GC oven's programming commenced with a base temperature of 40 °C, held steady for 2 minutes, followed by a progressive increase to a final temperature of 320°C at a gradient of 4°C per minute. The rate of flow for the helium gas within the column was sustained at 1.4 cm^2/sec. As for the mass spectrometer detector (MSD) conditions, an EI ionization source of 70 eV was used, with a mass range spanning from 45–600 atomic mass units (amu). The multiplier voltage was set to 2341 V, with the ion-source temperature maintained at 230 °C.

The polycyclic aromatic hydrocarbons (PAHs) were recognized by aligning the distinct mass spectra with existing literature and the National Institute of Standards and Technology (NIST) database. In order to evaluate the quantity of PAHs present within the samples, an external calibration curve was generated. This was based on analytical standards with a range of concentrations (n=8), incorporating the Sigma CRM47930 PAHs mix with concentrations of 50, 100, 200, 300, 400, 600, 800, and 1200 ng/mL. Several indices related to PAHs were determined to aid in the quantification and understanding of the varied origins contributing to the organic content in the system.

Wind Trajectory Analysis

To track the wind direction, we used the Hybrid Single-Particle Lagrangian Integrated Trajectory model (HYSPLIT) (Draxler and Hess, 1998). This computer model is widely used to forecast wildfire smoke trajectories as it can impact air quality and human health. It also has archival data of the movement of air parcels. This archival information was combined with two functions of the model – 1. Forward trajectory that gives the direction the air parcel moved from a given point of interest and 2. Backward trajectory that gives the direction from which air parcels came to the point of interest. In our case, we used forward trajectories for the fire locations to see the direction of potential charcoal transport and backward trajectories on sampling locations to see the potential sources of charcoal particles deposited. The model was run on all days starting from 22nd February to the date of sample collection. It was run for 24 hours each day with new trajectories starting every 2 hours. Since this was a large fire, we considered wind parcels at

different altitudes ranging from 100 meters to 1 kilometer from the ground level. We also collected wind speed and wind direction data from Kargudi weather station, about 2 km and 4 km southeast of Ombetta and Imbrella, respectively. The Kargudi weather Station is close to the fire patch in MTR (~5 km) (fig 1).

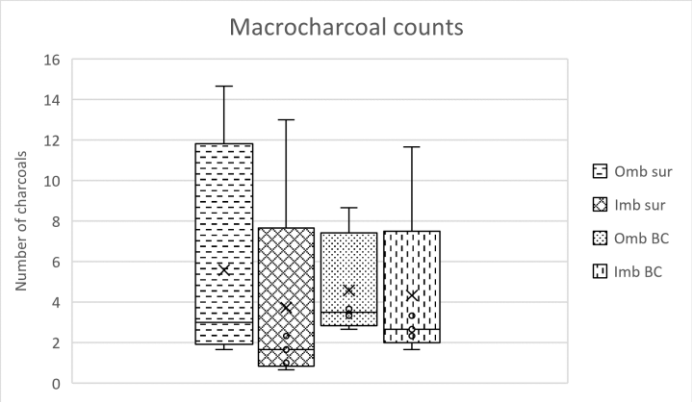

Fig 2: Box plot of macrocharcoal counts per gram of soil. Three extracts were done for each sample. The mean, median, maximum and minimum values of charcoal obtained are given in this plot. For all the samples, average number of charcoals lies between 4 and 6.

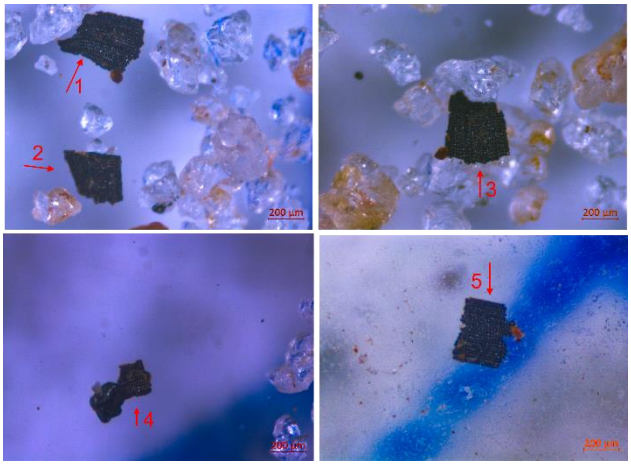

Fig 3 macrocharcoal particles (red arrows) found from the wetland samples. Only macrocharcoal of this type was found from the samples. This according to Mustaphi and Pisaric, 2014's classification scheme is of wood origin. The W/L ratio of these charcoals also show that they are of wood origin. The transparent crystals surrounding the charcoals are quartz. The W/L ratio of 1, 2,3 ,4 and 5 are 0.95, 0.80,

Results

Macro and Microcharcoal

Macrocharcoal counts of both sets of samples, surface and bottle core, were disproportionately low compared to the range and extent of the forest fire (see fig 2). The maximum number of macrocharcoal counted was 15 from one Ombetta surface sample, while the average number of particles was ~5 for all samples from both the wetlands. All the charcoal particles observed have

a textured broad shape indicative of wood burning (Mustaphi and Pisaric, 2014) (fig 3). The width to length ratio of all these particles are >0.5 which again indicates a woody origin (Aleman et al., 2013) (fig 3). Macrocharcoal counting of the top 5 cm of Town Vayal (TV), another wetland from a very low fire frequency area of Mudumalai was also done. This top layer sample had 13 charcoals per gram of sample. This sample also had morphologically similar type of macrocharcoal in them. Microcharcoal to pollen (C/P) ratio was 1.2 and 1.1 for Ombetta and Imbrella respectively. Length to width ratio of the microcharcoals gave values ranging from 1.2 (leaf) to >2.13 (wood) to >3.62 (grass) (Cui et al., 2009) (fig 4). Thus, vegetation of all types is represented in the pollen slides while only wood charcoals are represented in the macrocharcoal.

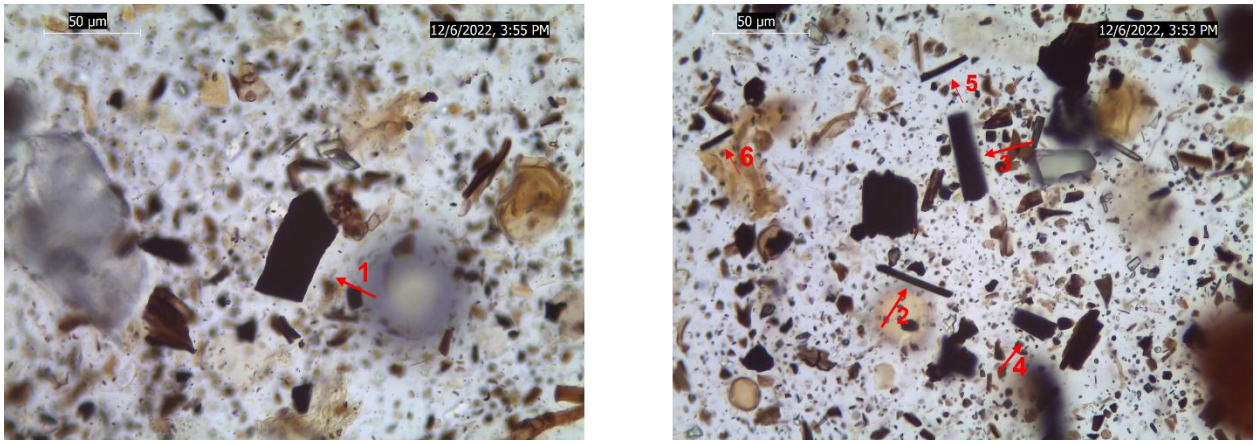

Fig 4: microcharcoal images of the wetland samples. The red arrows show the microcharcoal. Unlike macrocharcoal, microcharcoal of all sizes are found in the sample. *The L/W values of 1,2,3,4,5, and 6 are 1.97, 12.3, 3.90, 2.19, 1.22, and 6.55*

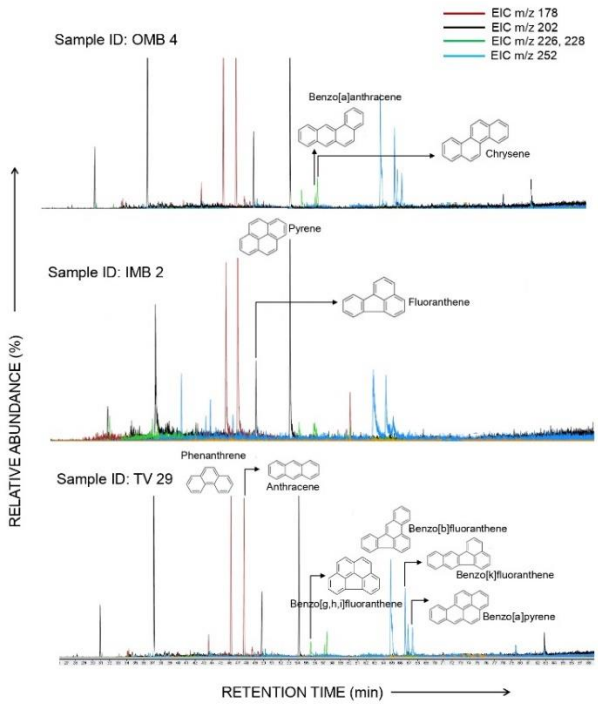

Fig 5: Chromatograms of the 10 PAHs obtained. These samples are representative of all the samples analysed. OMB and IMB are the wetland samples and TV29 is a surface sample from a low fire-frequency area of MTR. The PAHs found include phenanthrene, anthracene, fluoranthene, pyrene, benzo[g,h,i]fluoranthene, benz[a]anthracene, chrysene, benzo[b]fluoranthene, and benzo[a]pyrene, shown in the figures with representative peak positions.

PAH Analysis

Out of the 32 PAH compounds reported in literature (Dzepina et al., 2007), 10 compounds were detected from the nine surface samples of the wetlands (fig 5) . This includes four Low Molecular Weight (LMW) ones, phenanthrene, anthracene, fluoranthene and pyrene and six High Molecular Weight (HMW) ones, benzo[g,h,i]fluoranthene, benz[a]anthracene, Chrysene, benzo[b]fluoranthene, and benzo[a]pyrene. All the Imbrella samples are missing benzo[g,h,i]fluoranthene and benz[a]anthracene except for IMB 4 and IMB 5 respectively. LMW/ total PAH value shows that Ombetta has low LMW/ΣPAHs (mean ~0.37) while Imbrella has comparatively high values (mean ~0.74). However, Imbrella is generally low in PAHs (mean of total PAHs ~0.76 ng/g) compared to Ombetta (mean of total PAHs ~3.5 ng/g). Imbrella also lacks many of the higher end compounds. The ΣLMW PAHs of Imbrella is also low compared to Ombetta. Ombetta is rich in HMW PAHs (avg ~0.63). Furthermore, Town Vayal surface sample, which is from a low fire-frequency area, also yielded the same 10 compounds and is rich in LMW compounds (>80% of total PAH detected). The ΣPAHs for town vayal is comparable to Ombetta (2.94 ng/g) but is generally rich in LMW PAHs than HMW unlike Ombetta.

Ratios of different PAHs were used to determine the source of PAHs. Yunker et al., 2002 show that samples with anthracene / (anthracene (Ant)+ phenanthrene (Ph)) ratio >0.1 are pyrogenic in origin. This value for Ombetta, Imbrella and Town Vayal lies between 0.75 - 0.81, 0.38-0.61 and 0.69 respectively. Similarly, for the Fluoranthene (Fla) / (fluoranthene + pyrene (Py)) ratio >0.5 indicate pyrogenic source. This value lies between 0.53-0.61,0.4-0.63, and 0.58 for Ombetta, Imbrella and town vayal respectively. One sample of Imbrella (IMB 1) shows petrogenic signature, while rest of the samples including the town vayal are pyrogenic in origin (Fig 6a). Ratios of Fla/Py vs Ph/Ant (Fig 6b) and Fla/ Py vs LMW/HMW (Fig 6c) (Ranjbar Jafarabadi et al., 2017) also suggest pyrogenic source for all the samples except for town vayal which has a high LMW/HMW value (Fig 6c).

Table 1 PAH analysis summary

Site	Σ PAH	Σ LMW	ΣHMW	a/(a+p)	f/(f+p)	LMW/HMW	f/p
IMB	0.764637	100277	41398	0.5614	0.56	0.863	1.34
OMB	3.5893	242044	432627	0.7802	0.58	0.592	1.39
TV	2.9468	427586	125852	0.6925	0.58	3.397	1.40

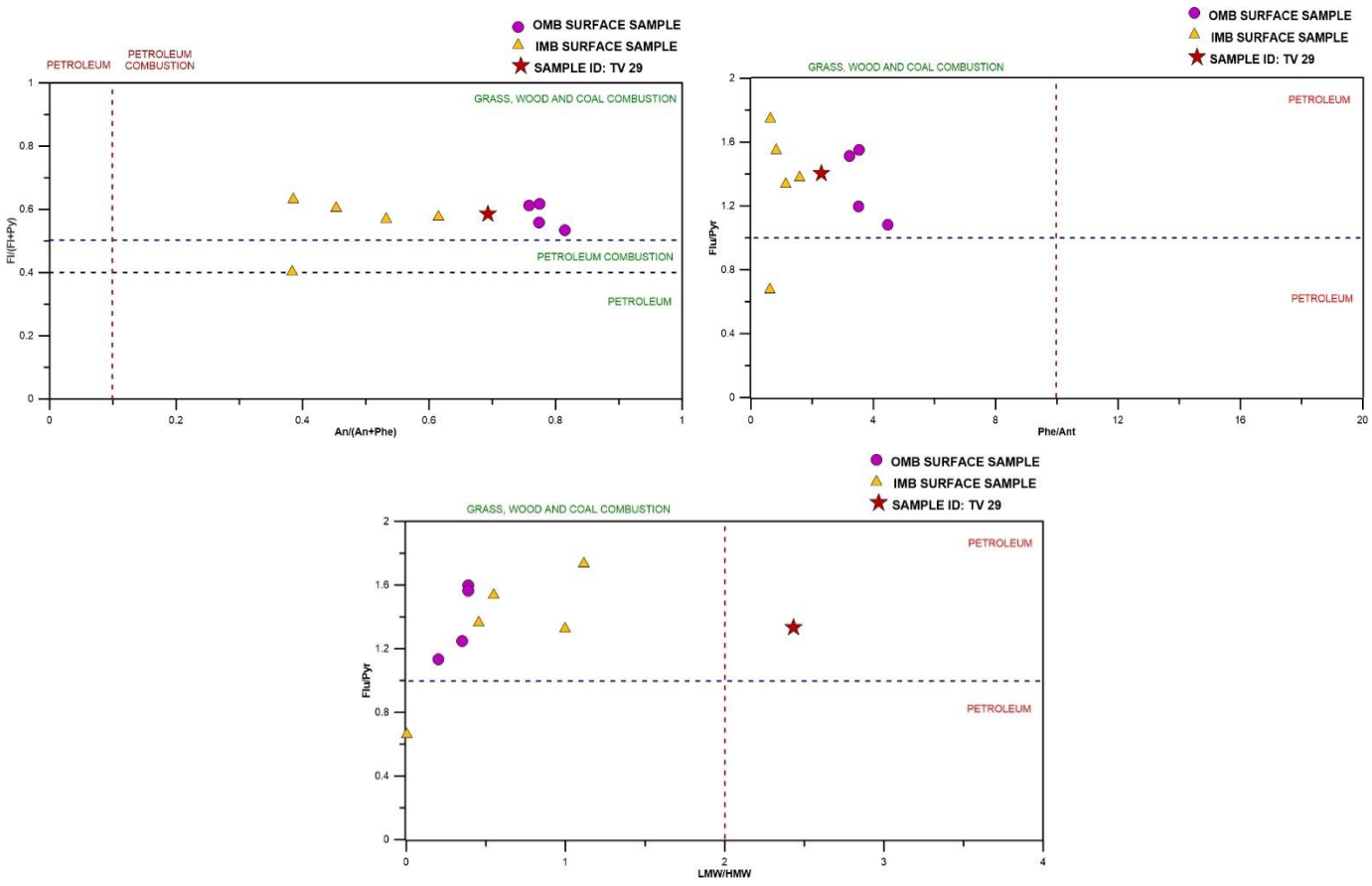

Fig 6: PAH source determination plots

Wind Trajectory Analysis

From the Kargudi weather station data, we created a wind rose diagram to observe the general wind pattern during and after the fire events (fig 7). During the fire event (22 – 26 February 2019), the weather station recorded a wind speed ranging from 0.3 to 18.3 km/hr. The wind rose diagram (fig 7) showed that winds with speed greater than 9.3 km/hr dominated these days. More than 60% of the winds were from the Northeast, East or Southeast and thus in general, easterly in direction. This seems to have aided the spread of the fire towards the west. The westerly winds start to get stronger towards the end of the fire event. After the fire event, from 27 February 2019, wind speed ranged between 0.3 to 12.3 km/hr, more than 65% of the wind was westerly.

HYSPLIT model was used to look at wind trajectories every hour of the day at different heights from the surface. The forward trajectory models from the major fire locations were created. The results show that wind from the larger Bandipur fire patch did not pass through any of the sample locations both during and after the fire event except on 6 March, 2019, one day before the sample collection. Forward trajectory models on the smaller MTR fire patch show that the wind was passing through the sample locations both during and after the fire days. This implies that whatever fire proxies were captured by the wetlands would be dominated by the MTR fire source. A backward trajectory of the wind parcels at the sample locations was also analyzed that confirmed the conclusions from the forward trajectory models (REF Supplementary material (III)).

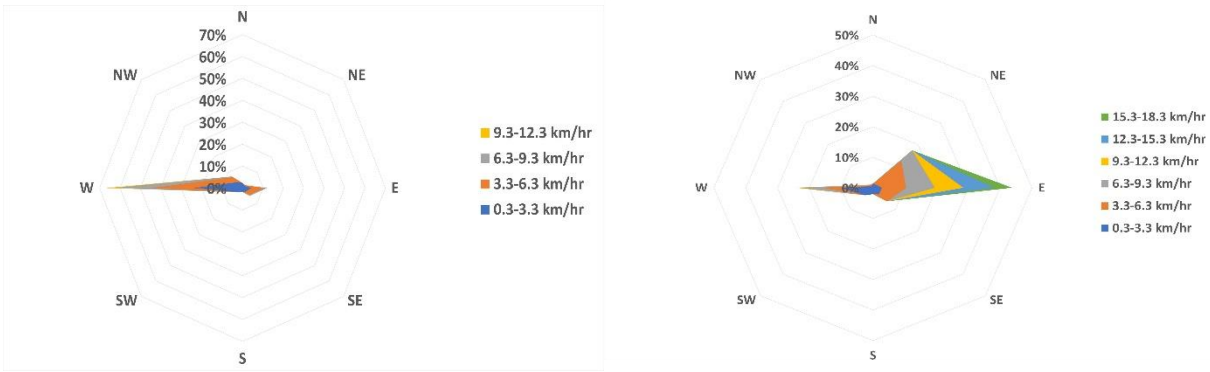

Fig 7: Wind rose diagram created from the Kargudi weather station data. The left side image is after fire (27th feb to 7 of march, 2019). Right side image is from 22nd feb to 26th feb, 2019, when the fire was prominent. During the fire days the wind was mostly westerly. More than 40% of them are high speed wind (15.3-18.3 km/hr). Easterly winds start to develop towards the end of fire. After the fire event, the wind is mostly from the east with speed ranging 12.3-6.3 km/hr. The change in wind direction has in fact helped in curbing the fire.

Discussion

Macrocharcoal and Microcharcoal Count

Macrocharcoal counts from both wetlands are low (mean ~5) for all the samples. Whitlock and Larsen (2002), in their study, show that macrocharcoal count >50 was indicative of fire events. However, we must note that tropical forests are not included in this study and hence this arbitrary value may not be applicable to our study from tropical India. Since ours is the first study to try and evaluate fire-proxy relationships in the dry tropical forests of India, we do not yet have baseline values for a fire peak representation in surface sediments in this landscape. Hence we chose to compare our results to investigations on sediment cores from the larger region of the Western Ghats (Bhagwat et al., 2012, 2014; Kulkarni et al., 2021; Nogué et al., 2018) and a surface sample (top 5cm) from Town vayal. These investigations on fire-vegetation-human inter-relationships have been done in the Kodagu district of Karnataka, central Western Ghats in anthropogenically modified landscapes, albeit in tropical wet evergreen forests and very low burning part of the Mudumalai Tiger reserve, respectively. On one of the sediment cores, the authors report an increase of fire in two time periods: ~1800-1400 yr BP and 400-0 yr BP, was represented by 61 charcoal particles per cm^3 of sample (Bhagwat et al., 2012; Kulkarni et al., 2021) respectively. This shows that >50 charcoal count for fire indication may hold for tropical India as well. However further study has to be done to confirm this. The surface of these sediment core had about 18 charcoals per cm^3 of sample. This low count is not very surprising as the region is very unlikely to burn as it is a plantation area. This strongly implies that the surface of our wetlands is not representative of the large surface fire. The understanding that macrocharcoal as a result of their larger size and limited mobility would only be able to travel small distances and represent a local fire event aligns well with our findings as both the wetlands are 5-7 kms away from either of the fire patches (Clark, 1988; Mooney and Tinner, 2011).

Macrocharcoal: Morphology

The Bandipur fire was one of the largest recent forest fires and burnt large swathes of the forest, including canopy trees and understory vegetation – both grass and shrub. Yet, only macrocharcoal, possibly of woody plants origin, were found (irregular, opaque with textured surface), while charcoal from the other vegetation types were not found. However, microcharcoal indicative of diverse vegetation types were found in the samples (based on the large range of sizes and shapes (Fig 4). Macrocharcoal of similar morphology is also found from the low burning, 800-year, old Town Vayal sample (unpublished data) as well from its surface. Thus, the presence of this macrocharcoal in both low burning location and >7km from the fire edge (OMB and IMB) shows that it can travel larger distances. It could also be distinctive of the tropical dry deciduous forest.

Polycyclic Aromatic Hydrocarbons (PAHs)

All of our wetland samples show pyrogenic source for the PAHs (fig 6). TV is more proximate to human occupation; it is likely that the signatures of PAHs there are of a mixed pyro-petrogenic origin. The higher LMW/HMW value for TV sample would be indicative of that. However, since the sample was collected in what is well within Tiger Reserve boundaries, we expect that most of the PAHs would be of pyrogenic origin for the purposes of this study.

The individual PAH compounds can give an idea of the spatial distribution of the fire (Vachula et al., 2022). According to Vachula et al., 2022, naphthalene, anthracene, acenaphthylene, and fluorine record local fire histories (within 40km) whereas phenanthrene, benzo[g,h,i] perylene, chrysene, benzo[k]fluoranthene, benzo[b]fluoranthene record both local and regional fires. Our samples are rich in compounds that can record both local and regional fires and thus indicate that the big near fire event was not well captured by the wetland.

LMW/ΣPAH is found to show a positive correlation with accumulation rate of sedimentary macrocharcoal of all size classes (Vachula et al., 2022). They thus postulate that the adsorption of PAHs (LMWs) to charcoal can be an important mode of transport and deposition for them.

However, (Kong et al., 2021) in their study of the peat samples from Malaysia observed a positive correlation of the HMW PAHs with charcoal abundance. The LMW was in fact decreasing with increasing charcoal abundance. In our case, both the wetlands and Town Vayal core top have low charcoal counts. While Town Vayal shows a high LMW/ΣPAH, Ombetta is rich in HMW PAHs. This difference in concentration of LMW and HMW in low charcoal scenario highlights the possibility for more research in linking either of these PAHs with charcoal abundance. Based on our results neither of the PAHs show any relationship with macrocharcoal. This indicates that the increase in concentration is independent of adsorption to charcoal as a transportation mechanism.

HMW PAHs are produced more in a high temperature scenario (McGrath et al., 2003). Forest fires, depending on the fuel that is burned and the climate, can be highly variable in terms of temperature of burning. Even though both Ombetta and Imbrella are close to each other (~3km), there is a huge distinction between them in terms of the PAH that were captured (LMW vs HMW). Imbrella is closer to the bigger fire patch. However, the Σ PAHs that got captured by the wetland is low compared to Ombetta. This shows that the signals from the bigger BTR patch were not captured by the wetland. HYSPLIT model also confirms that none of the wind parcel from the BTR passed through our sample locations. The high value of HMWs in Ombetta (Ombetta is closer to MTR patch) indicates that the signal might be from the MTR patch. HYSPLIT model results show that some of the winds did go through our sample location (Ombetta).

High percentages of LMW PAHs compared to HMW PAHs in the wet forest sediments of Town vayal shows that they can travel farther and get deposited. Their presence in low amounts even in Imbrella shows that they can get deposited in less transport-favorable environments as well. The LMW PAHs have low gas-particle partition coefficient (Alam et al., 2014; Xie et al., 2014) and so they are mostly associated with gas phase(Wang et al., 2016). This property of the LMW PAHs makes sense with their long range of transport. The opposite is true for HMW PAHs. Thus, high percentages of HMW PAHs in Ombetta and absence/ low concentration in both Imbrella and Town Vayal shows that they are more local fire indicators and are particle or transport medium dependent. However, more modern-day calibration has tinbe done on this regard before using them as reliable fire proxies.

According to Wang et al., 2016, PAH flux deposition of LMW PAHs (2 + 3 rings) are high with wet condition. This is because the LMWs are more water soluble (Mackay and Shiu, 1977) and tend to be associated more with gaseous phase. The HMW PAHs (4+5+6 rings) on the other hand, favor dry deposition. The PAH flux deposition was also found to be high on a calm day (Wang et al., 2016). In our case, from the fire start day to the day of sample collection, the climate was dry and windy. So, most of the LMW PAHs might have been carried away by the wind as they are more associated with the gaseous phase. Thus, the dry deposition mode should have been more favored in such conditions. However, the absence of HMW PAHs in Imbrella shows that wind does determine their transport and deposition just as is the case for macrocharcoal.

Conclusion

From our opportunistic sampling of wetland surfaces following a large fire event, we report the following important findings. First, we demonstrate the importance of wind direction in proxy transport and deposition. We see that all fire proxies considered in both wetlands – macrocharcoal, microcharcoal/pollen ratio and PAHs is disproportionately low and not representative of one of the largest forest fire events in the recent past in India. This is ascribed to the lack of favorable wind for deposition of these proxies. Second, the distance travelled by macrocharcoal (blocky texture) in our study site. For the smaller burnt area whose downwind fire proxies we seem to have captured through our sampling of these two wetland surfaces, charcoal particles of size 120-200 μ has been transported up to 7 km which to our knowledge is reported for the first time in India. Third, we report ambiguity in the use of PAH as fire proxy. HMW PAHs seem to capture local and high intensity fire well while LMW PAHs seem to be regional in nature. We also report ambiguity with respect to transportation and preservation of PAHs and their relationship with wet and dry deposition events. More modern-day fire calibration is required to have a more nuanced understanding of the factors that affect fire proxy transport and deposition and to reconstruct past fire events with more confidence.

References

Ajay K, Behera D, Bhattacharya S, Mishra PK, Ankit Y and Anoop A (2021) Distribution and characteristics of microplastics and phthalate esters from a freshwater lake system in Lesser Himalayas. *Chemosphere* 283: 131132: doi:10.1016/j.chemosphere.2021.131132.

Alam MS, Delgado-Saborit JM, Stark C and Harrison RM (2014) Investigating PAH relative reactivity using congener profiles, quinone measurements and back trajectories. *Atmospheric Chemistry and Physics* 14(5): 2467–2477: doi:10.5194/acp-14-2467-2014.

Aleman JC, Blarquez O, Bentaleb I, Bonté P, Brossier B, Carcaillet C, et al. (2013) Tracking land-cover changes with sedimentary charcoal in the Afrotropics. *The Holocene* 23(12): 1853–1862: doi:10.1177/0959683613508159.

Andreola F, Castellini E, Manfredini T and Romagnoli M (2004) The role of sodium hexametaphosphate in the dissolution process of kaolinite and kaolin. *Journal of the European Ceramic Society* 24(7): 2113–2124: doi:10.1016/S0955-2219(03)00366-2.

Anupama K, Prasad S and Reddy CS (2014) Vegetation, land cover and land use changes of the last 200 years in the Eastern Ghats (southern India) inferred from pollen analysis of sediments from a rain-fed tank and remote sensing. *Quaternary International* 325: 93–104: doi:10.1016/j.quaint.2014.02.003.

Archibald S, Staver AC and Levin SA (2012) Evolution of human-driven fire regimes in Africa. *Proceedings of the National Academy of Sciences* 109(3): 847–852: doi:10.1073/pnas.1118648109.

Argiriadis E, Battistel D, McWethy DB, Vecchiato M, Kirchgeorg T, Kehrwald NM, et al. (2018) Lake sediment fecal and biomass burning biomarkers provide direct evidence for prehistoric human-lit fires in New Zealand. *Scientific Reports* 8(1): 12113: doi:10.1038/s41598-018-30606-3.

Beerling D (2007) *The Emerald Planet: How Plants Changed Earth's History*. Oxford University Press.

Behera D, Bhattacharya S, Rahman A, Kumar S and Anoop A (2022) Molecular tracers for characterization and distribution of organic matter in a freshwater lake system from the Lesser Himalaya. *Biogeochemistry* 161(3): 315–334: doi:10.1007/s10533-022-00984-y.

Bennett KD (1990) Textbook of pollen analysis. K. FAEGRI, J. IVERSEN (4th edn by K. FAEGRI, P. E. KALAND, K. KRZYWINSKI), Publisher John Wiley and Sons, Chichester 1989 (328 pp) £51.00 ISBN 0 471 92178 5. *Journal of Quaternary Science* 5(3): 254–255: doi:10.1002/jqs.3390050310.

Berner RA (2006) GEOCARBSULF: A combined model for Phanerozoic atmospheric O2 and CO2. *Geochimica et Cosmochimica Acta* 70(23): 5653–5664: doi:10.1016/j.gca.2005.11.032.

529 Bhagwat SA, Nogué S and Willis KJ (2012) Resilience of an ancient tropical forest landscape to
530 7500years of environmental change. *Biological Conservation* 153: 108–117:
531 doi:10.1016/j.biocon.2012.05.002.

532 Bhagwat SA, Nogué S and Willis KJ (2014) Cultural drivers of reforestation in tropical forest
533 groves of the Western Ghats of India. *Forest Ecology and Management* 329: 393–400:
534 doi:10.1016/j.foreco.2013.11.017.

535 Blumer M (1976) Polycyclic Aromatic Compounds in Nature. *Scientific American* 234(3): 34–45:
536 doi:10.1038/scientificamerican0376-34.

537 Bowman DM (2015) What is the relevance of pyrogeography to the Anthropocene? *The*
538 *Anthropocene Review* 2(1): 73–76: doi:10.1177/2053019614547742.

539 Bowman DMJS, Balch J, Artaxo P, Bond WJ, Cochrane MA, D'Antonio CM, et al. (2011) The
540 human dimension of fire regimes on Earth: The human dimension of fire regimes on Earth.
541 *Journal of Biogeography* 38(12): 2223–2236: doi:10.1111/j.1365-2699.2011.02595.x.

542 Bowman DMJS, Balch JK, Artaxo P, Bond WJ, Carlson JM, Cochrane MA, et al. (2009) Fire in
543 the Earth System. *Science* 324(5926): 481–484: doi:10.1126/science.1163886.

544 Burns WA, Mankiewicz PJ, Bence AE, Page DS and Parker KR (1997) A principal-component
545 and least-squares method for allocating polycyclic aromatic hydrocarbons in sediment to
546 multiple sources. *Environmental Toxicology and Chemistry* 16(6): 1119–1131:
547 doi:10.1002/etc.5620160605.

548 Chennabasaveshwar P (2019) What Caused the Fire Bandipur Forest? , 25 February. Available
549 at: https://www.oneindia.com/india/what-caused-fire-in-bandipur-forest-2856666.html?story=2;

550 Clark JS (1988) Particle Motion and the Theory of Charcoal Analysis: Source Area, Transport,
551 Deposition, and Sampling. *Quaternary Research* 30(1): 67–80: doi:10.1016/0033-
552 5894(88)90088-9.

553 Clark JS, Lynch J, Stocks BJ and Goldammer JG (1998) Relationships between charcoal
554 particles in air and sediments in west-central Siberia. *The Holocene* 8(1): 19–29:
555 doi:10.1191/095968398672501165.

556 Conedera M, Tinner W, Neff C, Meurer M, Dickens AF and Krebs P (2009) Reconstructing past
557 fire regimes: methods, applications, and relevance to fire management and conservation.
558 *Quaternary Science Reviews* 28(5–6): 555–576: doi:10.1016/j.quascirev.2008.11.005.

559 Cui Q, Marquer L, Arzarello M and Lebreton V (2009) An attempt to separate anthropic and
560 natural fire signals in an archaeological context-The case of the Mousterian site Grotta Reali
561 (Rocchetta a Volturno Molise, Central Italy). *Frontiers of Earth Science in China* 3(2): 171–174:
562 doi:10.1007/s11707-009-0014-8.

563 D. Burton F (2009) *Fire: The Spark That Ignited Human Evolution*. .

564 deMenocal PB (2004) African climate change and faunal evolution during the Pliocene–
565 Pleistocene. *Earth and Planetary Science Letters* 220(1–2): 3–24: doi:10.1016/S0012-
566 821X(04)00003-2.

Denis EH, Toney JL, Tarozo R, Scott Anderson R, Roach LD and Huang Y (2012) Polycyclic aromatic hydrocarbons (PAHs) in lake sediments record historic fire events: Validation using HPLC-fluorescence detection. *Organic Geochemistry* 45: 7–17: doi:10.1016/j.orggeochem.2012.01.005.

Draxler RR and Hess GD (1998) NOAA Technical Memorandum ERL ARL-224. .

Duffin KI, Gillson L and Willis KJ (2008) Testing the sensitivity of charcoal as an indicator of fire events in savanna environments: quantitative predictions of fire proximity, area and intensity. *The Holocene* 18(2): 279–291: doi:10.1177/0959683607086766.

Dunbar RIM (2009) Richard Wrangham, Catching Fire: How Cooking Made Us Human: Basic Books, New York, 2009, $26.95. *Human Nature* 20(4): 447–449: doi:10.1007/s12110-009-9075-3.

Dzepina K, Arey J, Marr LC, Worsnop DR, Salcedo D, Zhang Q, et al. (2007) Detection of particle-phase polycyclic aromatic hydrocarbons in Mexico City using an aerosol mass spectrometer. *International Journal of Mass Spectrometry* 263(2–3): 152–170: doi:10.1016/j.ijms.2007.01.010.

Edwards NT (1983) Polycyclic Aromatic Hydrocarbons (PAH's) in the Terrestrial Environment—A Review. *Journal of Environmental Quality* 12(4): 427–441: doi:10.2134/jeq1983.00472425001200040001x.

Enache MD and Cumming BF (2006) Tracking recorded fires using charcoal morphology from the sedimentary sequence of Prosser Lake, British Columbia (Canada). *Quaternary Research* 65(02): 282–292: doi:10.1016/j.yqres.2005.09.003.

Feurdean A (2021) Experimental production of charcoal morphologies to discriminate fuel source and fire type: an example from Siberian taiga. *Biogeosciences* 18(12): 3805–3821: doi:10.5194/bg-18-3805-2021.

Flannigan M, Stocks B, Turetsky M and Wotton M (2009) Impacts of climate change on fire activity and fire management in the circumboreal forest. *Global Change Biology* 15(3): 549–560: doi:10.1111/j.1365-2486.2008.01660.x.

Foley SF, Gronenborn D, Andreae MO, Kadereit JW, Esper J, Scholz D, et al. (2013) The Palaeoanthropocene – The beginnings of anthropogenic environmental change. *Anthropocene* 3: 83–88: doi:10.1016/j.ancene.2013.11.002.

Frank-DePue L, Vachula RS, Balascio NL, Cahoon K and Kaste JM (2022) Trends in sedimentary charcoal shapes correspond with broad-scale land-use changes: insights gained from a 300-year lake sediment record from eastern Virginia, USA. *Journal of Paleolimnology*. Available at: https://link.springer.com/10.1007/s10933-022-00260-x: doi:10.1007/s10933-022-00260-x.

Gedye SJ, Jones RT, Tinner W, Ammann B and Oldfield F (2000) The use of mineral magnetism in the reconstruction of fire history: a case study from Lago di Origlio, Swiss Alps. *Palaeogeography, Palaeoclimatology, Palaeoecology* 164(1–4): 101–110: doi:10.1016/S0031-0182(00)00178-4.

606 Glasspool IJ, Edwards D and Axe L (2004) Charcoal in the Silurian as evidence for the earliest
607 wildfire. *Geology* 32(5): 381: doi:10.1130/G20363.1.

608 Glikson A (2013) Fire and human evolution: The deep-time blueprints of the Anthropocene.
609 *Anthropocene* 3: 89–92: doi:10.1016/j.ancene.2014.02.002.

610 Gu Y, Pearsall DM, Xie S and Yu J (2007) Vegetation and fire history of a Chinese site in
611 southern tropical Xishuangbanna derived from phytolith and charcoal records from Holocene
612 sediments. *Journal of Biogeography* 0(0): 070821084123002-??? doi:10.1111/j.1365-
613 2699.2007.01763.x.

614 Gunnar E (1960) The acetolysis method-a revised description. *Sven Bot Tidskr* 516–564.

615 Herring JR (2013) Charcoal Fluxes into Sediments of the North Pacific Ocean: The Cenozoic
616 Record of Burning. In: Sundquist ET and Broecker WS (eds) *Geophysical Monograph Series*.
617 Washington, D. C.: American Geophysical Union, 419–442. Available at:
618 http://doi.wiley.com/10.1029/GM032p0419: doi:10.1029/GM032p0419.

619 Higuera P, Peters M, Brubaker L and Gavin D (2007) Understanding the origin and analysis of
620 sediment-charcoal records with a simulation model. *Quaternary Science Reviews* 26(13–14):
621 1790–1809: doi:10.1016/j.quascirev.2007.03.010.

622 Iyer V, Kawale S, Kotak V and Panchal M (2021) Mapping of forest fire area in Bandipur
623 National Park, India using Sentinel 2B and Landsat 8 satellite data. .

624 Jensen K, Lynch EA, Calcote R and Hotchkiss SC (2007) Interpretation of charcoal
625 morphotypes in sediments from Ferry Lake, Wisconsin, USA: do different plant fuel sources
626 produce distinctive charcoal morphotypes? *The Holocene* 17(7): 907–915:
627 doi:10.1177/0959683607082405.

628 Jia G, Peng P, Zhao Q and Jian Z (2003) Changes in terrestrial ecosystem since 30 Ma in East
629 Asia: Stable isotope evidence from black carbon in the South China Sea. *Geology* 31(12): 1093:
630 doi:10.1130/G19992.1.

631 Kong S-R, Yamamoto M, Shaari H, Hayashi R, Seki O, Mohd Tahir N, et al. (2021) The
632 significance of pyrogenic polycyclic aromatic hydrocarbons in Borneo peat core for the
633 reconstruction of fire history. *PLOS ONE* 16(9): e0256853: doi:10.1371/journal.pone.0256853.

634 Kulkarni C, Finsinger W, Anand P, Nogué S and Bhagwat SA (2021) Synergistic impacts of
635 anthropogenic fires and aridity on plant diversity in the Western Ghats: Implications for
636 management of ancient social-ecological systems. *Journal of Environmental Management* 283:
637 111957: doi:10.1016/j.jenvman.2021.111957.

638 Laflamme RE and Hites RA (1978) The global distribution of polycyclic aromatic hydrocarbons
639 in recent sediments. *Geochimica et Cosmochimica Acta* 42(3): 289–303: doi:10.1016/0016-
640 7037(78)90182-5.

641 Lawson IT, Tzedakis PC, Roucoux KH and Galanidou N (2013) The anthropogenic influence on
642 wildfire regimes: charcoal records from the Holocene and Last Interglacial at Ioannina, Greece.
643 *Journal of Biogeography* 40(12): 2324–2334: doi:10.1111/jbi.12164.

644 Lerch M, Unkelbach J, Schneider F, Zech M and Klinge M (2022) Holocene vegetation
645 reconstruction in the forest–steppe of Mongolia based on leaf waxes and macro-charcoals in
646 soils. *E&G Quaternary Science Journal* 71(1): 91–110: doi:10.5194/egqsj-71-91-2022.

647 Leys B, Brewer SC, McConaghy S, Mueller J and McLauchlan KK (2015) Fire history
648 reconstruction in grassland ecosystems: amount of charcoal reflects local area burned.
649 *Environmental Research Letters* 10(11): 114009: doi:10.1088/1748-9326/10/11/114009.

650 Leys B, Carcaillet C, Dezileau L, Ali AA and Bradshaw RHW (2013) A comparison of charcoal
651 measurements for reconstruction of Mediterranean paleo-fire frequency in the mountains of
652 Corsica. *Quaternary Research* 79(3): 337–349: doi:10.1016/j.yqres.2013.01.003.

653 Lu H, Zhu L and Zhu N (2009) Polycyclic aromatic hydrocarbon emission from straw burning
654 and the influence of combustion parameters. *Atmospheric Environment* 43(4): 978–983:
655 doi:10.1016/j.atmosenv.2008.10.022.

656 Lynch JA, Clark JS and Stocks BJ (2004) Charcoal production, dispersal, and deposition from
657 the Fort Providence experimental fire: interpreting fire regimes from charcoal records in boreal
658 forests. *Canadian Journal of Forest Research* 34(8): 1642–1656: doi:10.1139/x04-071.

659 MacDonald GM, Larsen CPS, Szeicz JM and Moser KA (1991) The reconstruction of boreal
660 forest fire history from lake sediments: A comparison of charcoal, pollen, sedimentological, and
661 geochemical indices. *Quaternary Science Reviews* 10(1): 53–71: doi:10.1016/0277-
662 3791(91)90030-X.

663 Mackay D and Shiu WY (1977) Aqueous solubility of polynuclear aromatic hydrocarbons.
664 *Journal of Chemical & Engineering Data* 22(4): 399–402: doi:10.1021/je60075a012.

665 Marlon JR, Bartlein PJ, Carcaillet C, Gavin DG, Harrison SP, Higuera PE, et al. (2009) Erratum:
666 Climate and human influences on global biomass burning over the past two millennia. *Nature*
667 *Geoscience* 2(4): 307–307: doi:10.1038/ngeo468.

668 McGrath TE, Chan WG and Hajaligol MR (2003) Low temperature mechanism for the formation
669 of polycyclic aromatic hydrocarbons from the pyrolysis of cellulose. *Journal of Analytical and*
670 *Applied Pyrolysis* 66(1–2): 51–70: doi:10.1016/S0165-2370(02)00105-5.

671 Mooney SD and Tinner W (2011) The analysis of charcoal in peat and organic sediments. 19.

672 Musa Bandowe BA, Srinivasan P, Seelge M, Sirocko F and Wilcke W (2014) A 2600-year
673 record of past polycyclic aromatic hydrocarbons (PAHs) deposition at Holzmaar (Eifel,
674 Germany). *Palaeogeography, Palaeoclimatology, Palaeoecology* 401: 111–121:
675 doi:10.1016/j.palaeo.2014.02.021.

676 Mustaphi CJC and Pisaric MFJ (2014) A classification for macroscopic charcoal morphologies
677 found in Holocene lacustrine sediments. *Progress in Physical Geography: Earth and*
678 *Environment* 38(6): 734–754: doi:10.1177/0309133314548886.

679 Nogué S, Tovar C, Bhagwat SA, Finsinger W and Willis KJ (2018) Exploring the Ecological
680 History of a Tropical Agroforestry Landscape Using Fossil Pollen and Charcoal Analysis from
681 Four Sites in Western Ghats, India. *Ecosystems* 21(1): 45–55: doi:10.1007/s10021-017-0132-1.

682 Pausas JG and Keeley JE (2009) A Burning Story: The Role of Fire in the History of Life.
683 *BioScience* 59(7): 593–601: doi:10.1525/bio.2009.59.7.10.

684 Pereboom EM, Vachula RS, Huang Y and Russell J (2020) The morphology of experimentally
685 produced charcoal distinguishes fuel types in the Arctic tundra. *The Holocene* 30(7): 1091–
686 1096: doi:10.1177/0959683620908629.

687 Pisaric MFJ (2002) [No title found]. *Journal of Paleolimnology* 28(3): 349–354:
688 doi:10.1023/A:1021630017078.

689 Ranjbar Jafarabadi A, Riyahi Bakhtiari A, Aliabadian M and Shadmehri Toosi A (2017) Spatial
690 distribution and composition of aliphatic hydrocarbons, polycyclic aromatic hydrocarbons and
691 hopanes in superficial sediments of the coral reefs of the Persian Gulf, Iran. *Environmental*
692 *Pollution* 224: 195–223: doi:10.1016/j.envpol.2017.01.080.

693 Rummery TA (1983) The use of magnetic measurements in interpreting the fire histories of lake
694 drainage basins. *Hydrobiologia* 103(1): 53–58: doi:10.1007/BF00028427.

695 Schumacher S and Bugmann H (2006) The relative importance of climatic effects, wildfires and
696 management for future forest landscape dynamics in the Swiss Alps: FUTURE FOREST
697 DYNAMICS IN THE SWISS ALPS. *Global Change Biology* 12(8): 1435–1450:
698 doi:10.1111/j.1365-2486.2006.01188.x.

699 Scott AC (2000a) The Pre-Quaternary history of fire. *Palaeogeography, Palaeoclimatology,*
700 *Palaeoecology* 164(1–4): 281–329: doi:10.1016/S0031-0182(00)00192-9.

701 Scott AC (2000b) The Pre-Quaternary history of fire. *Palaeogeography, Palaeoclimatology,*
702 *Palaeoecology* 164(1–4): 281–329: doi:10.1016/S0031-0182(00)00192-9.

703 Scott AC (2010) Charcoal recognition, taphonomy and uses in palaeoenvironmental analysis.
704 *Palaeogeography, Palaeoclimatology, Palaeoecology* 291(1–2): 11–39:
705 doi:10.1016/j.palaeo.2009.12.012.

706 Scott AC and Glasspool IJ (2006) The diversification of Paleozoic fire systems and fluctuations
707 in atmospheric oxygen concentration. *Proceedings of the National Academy of Sciences*
708 103(29): 10861–10865: doi:10.1073/pnas.0604090103.

709 Stephens SL, Skinner CN and Gill SJ (2003) Dendrochronology-based fire history of Jeffrey
710 pine - mixed conifer forests in the Sierra San Pedro Martir, Mexico. *Canadian Journal of Forest*
711 *Research* 33(6): 1090–1101: doi:10.1139/x03-031.

712 Stevenson J and Haberle S (2005) PALAEOWORKS TECHNICAL PAPERS 5. .

713 Tinner W, Hofstetter S, Zeugin F, Conedera M, Wohlgemuth T, Zimmermann L, et al. (2006)
714 Long-distance transport of macroscopic charcoal by an intensive crown fire in the Swiss Alps -
715 implications for fire history reconstruction. *The Holocene* 16(2): 287–292:
716 doi:10.1191/0959683606hl925rr.

717 Tinner W and Hu FS (2003) Size parameters, size-class distribution and area-number
718 relationship of microscopic charcoal: relevance for fire reconstruction. *The Holocene* 13(4):
719 499–505: doi:10.1191/0959683603hl615rp.

720 Tissot C, Chikini H and T.S N ((n.d.)) *Pollen of wet evergreen forests of the Western Ghats,*
721 *India*. .

722 Vachula RS (2021) A meta-analytical approach to understanding the charcoal source area
723 problem. *Palaeogeography, Palaeoclimatology, Palaeoecology* 562: 110111:
724 doi:10.1016/j.palaeo.2020.110111.

725 Vachula RS, Karp AT, Denis EH, Balascio NL, Canuel EA and Huang Y (2022) Spatially
726 calibrating polycyclic aromatic hydrocarbons (PAHs) as proxies of area burned by vegetation
727 fires: Insights from comparisons of historical data and sedimentary PAH fluxes.
728 *Palaeogeography, Palaeoclimatology, Palaeoecology* 596: 110995:
729 doi:10.1016/j.palaeo.2022.110995.

730 Vachula RS and Richter N (2018) Informing sedimentary charcoal-based fire reconstructions
731 with a kinematic transport model. *The Holocene* 28(1): 173–178:
732 doi:10.1177/0959683617715624.

733 Vachula RS, Russell JM, Huang Y and Richter N (2018) Assessing the spatial fidelity of
734 sedimentary charcoal size fractions as fire history proxies with a high-resolution sediment record
735 and historical data. *Palaeogeography, Palaeoclimatology, Palaeoecology* 508: 166–175:
736 doi:10.1016/j.palaeo.2018.07.032.

737 Wang Q, Liu M, Li Y, Liu Y, Li S and Ge R (2016) Dry and wet deposition of polycyclic aromatic
738 hydrocarbons and comparison with typical media in urban system of Shanghai, China.
739 *Atmospheric Environment* 144: 175–181: doi:10.1016/j.atmosenv.2016.08.079.

740 Whitlock C and Larsen C (2002) Charcoal as a Fire Proxy. In: Smol JP, Birks HJB, Last WM,
741 Bradley RS and Alverson K (eds) *Tracking Environmental Change Using Lake Sediments*.
742 Dordrecht: Springer Netherlands, 75–97. Available at: http://link.springer.com/10.1007/0-306-
743 47668-1_5: doi:10.1007/0-306-47668-1_5.

744 Xie M, Hannigan MP and Barsanti KC (2014) Gas/particle partitioning of n-alkanes, PAHs and
745 oxygenated PAHs in urban Denver. *Atmospheric Environment* 95: 355–362:
746 doi:10.1016/j.atmosenv.2014.06.056.

747 Yan H, Yan Z, Wang L, Hao Z and Huang J (2022) Toward understanding submersed
748 macrophyte Vallisneria natans-microbe partnerships to improve remediation potential for PAH-
749 contaminated sediment. *Journal of Hazardous Materials* 425: 127767:
750 doi:10.1016/j.jhazmat.2021.127767.

751 Yan Z, Song N, Wang C and Jiang H (2021) Functional potential and assembly of microbes
752 from sediments in a lake bay and adjoining river ecosystem for polycyclic aromatic hydrocarbon
753 biodegradation. *Environmental Microbiology* 23(2): 628–640: doi:10.1111/1462-2920.15104.

754 Yang C-R, Lin T-C and Chang F-H (2007) Particle size distribution and PAH concentrations of
755 incense smoke in a combustion chamber. *Environmental Pollution* 145(2): 606–615:
756 doi:10.1016/j.envpol.2005.10.036.

757 Yunker MB, Macdonald RW, Vingarzan R, Mitchell RH, Goyette D and Sylvestre S (2002) PAHs
758 in the Fraser River basin: a critical appraisal of PAH ratios as indicators of PAH source and
759 composition. *Organic Geochemistry* 33(4): 489–515: doi:10.1016/S0146-6380(02)00002-5.

760

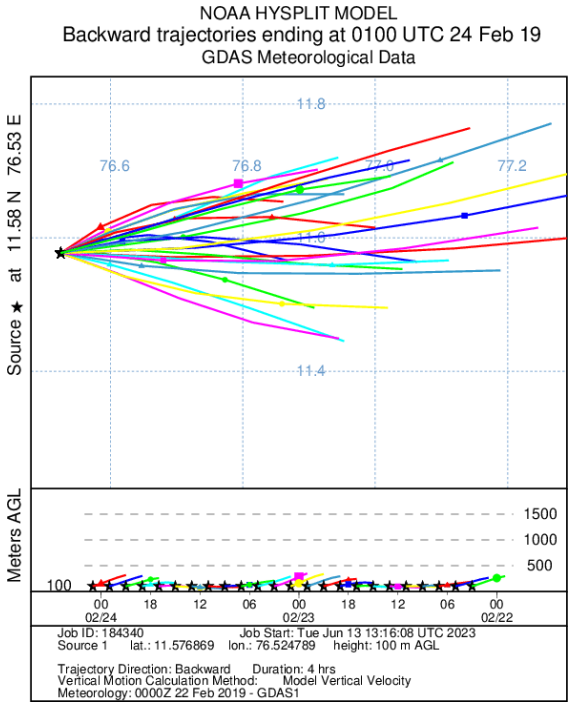

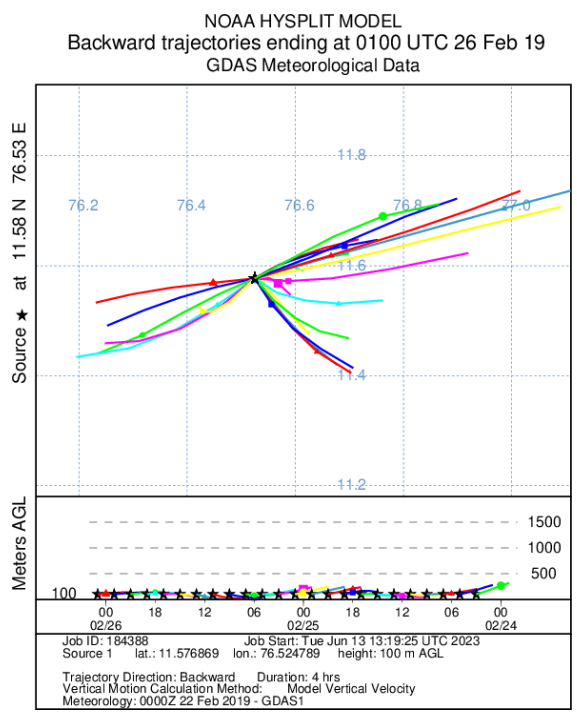

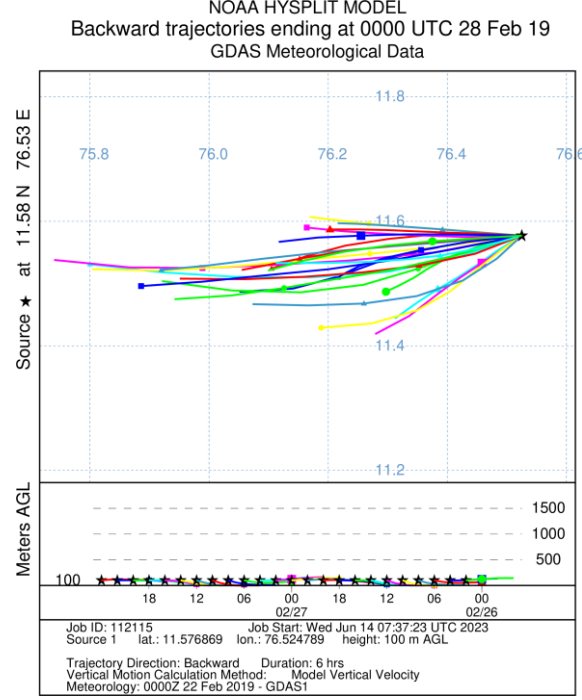

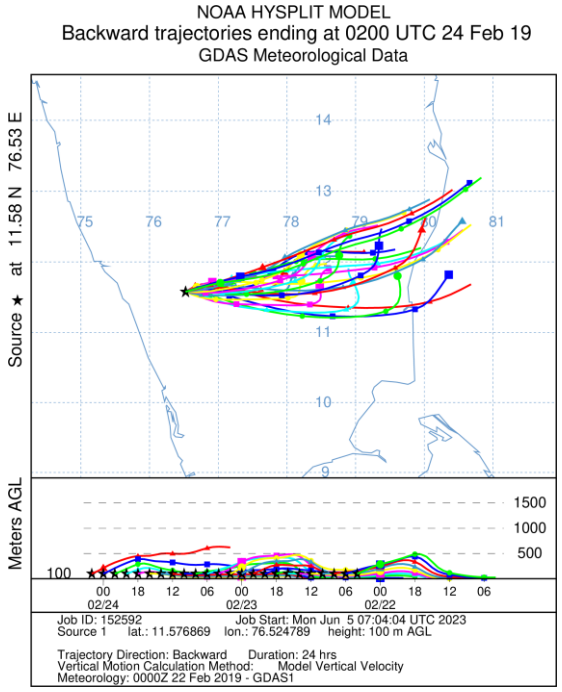

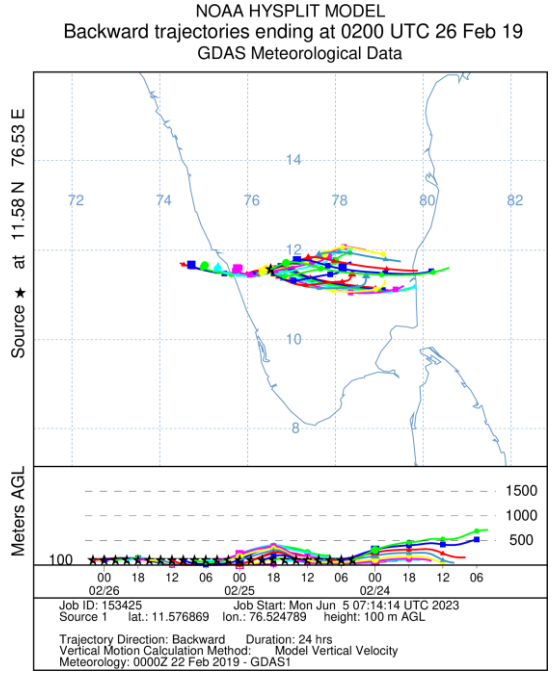

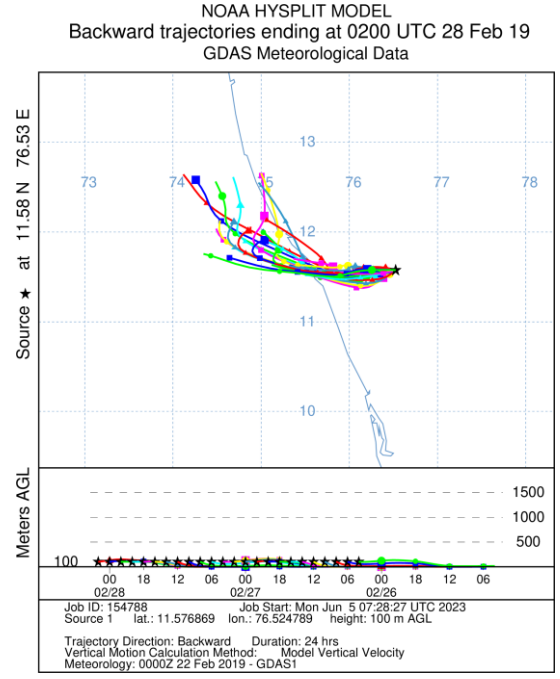

Backward wind trajectory map of Ombetta from 22-28 February, 2019, 100m above seal level. The top pictures show the magnified image of the trajectories.

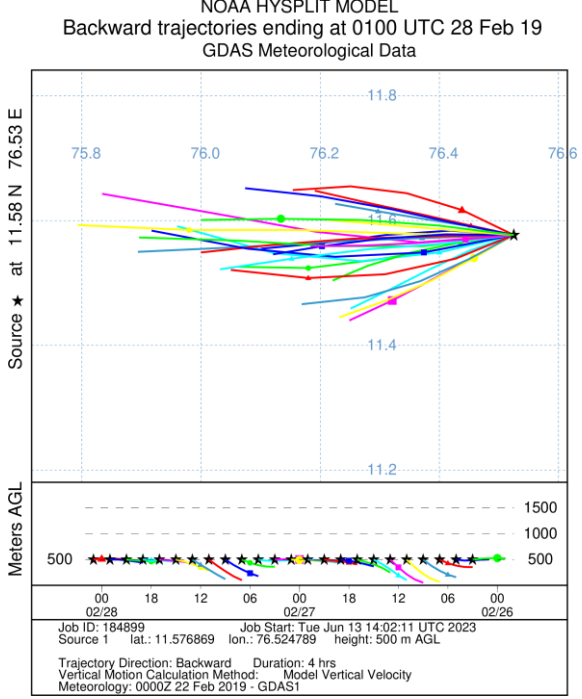

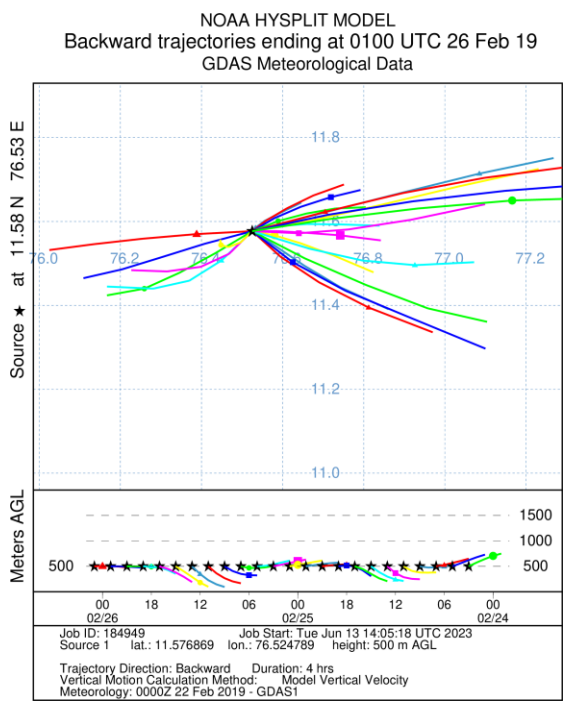

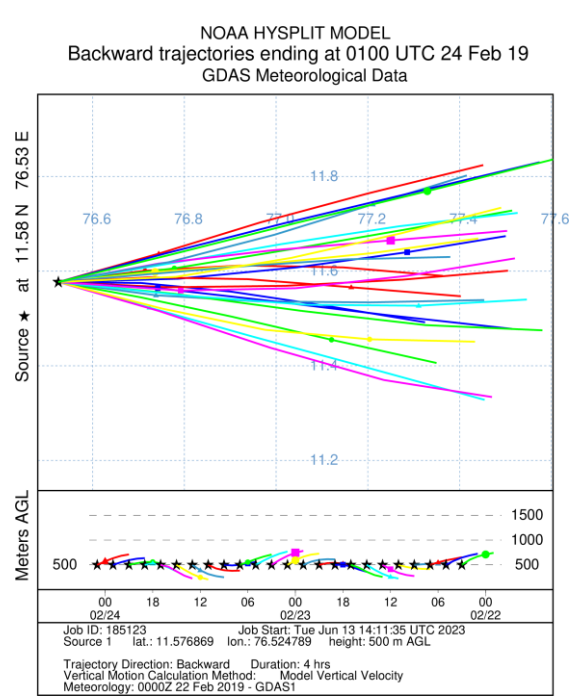

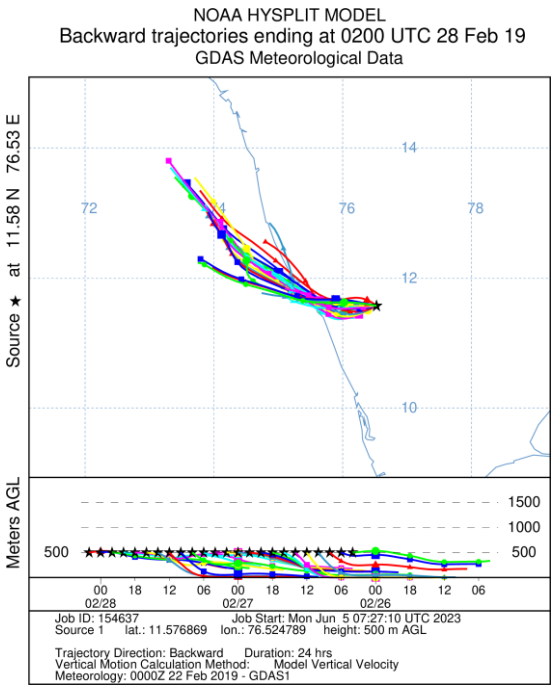

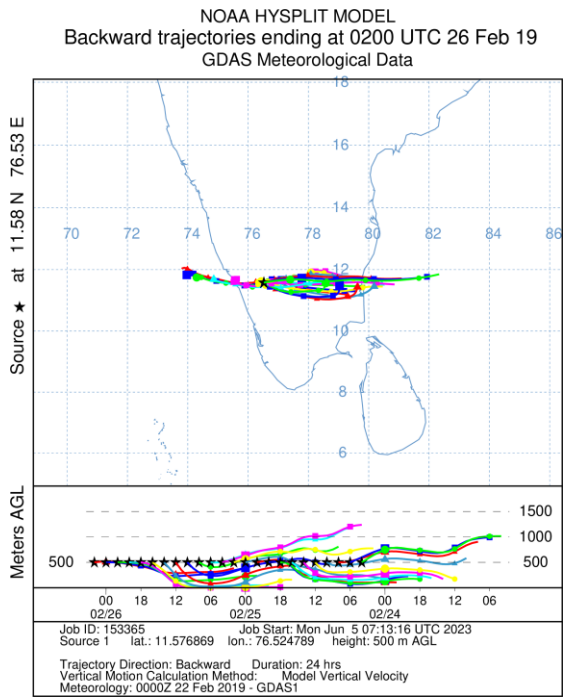

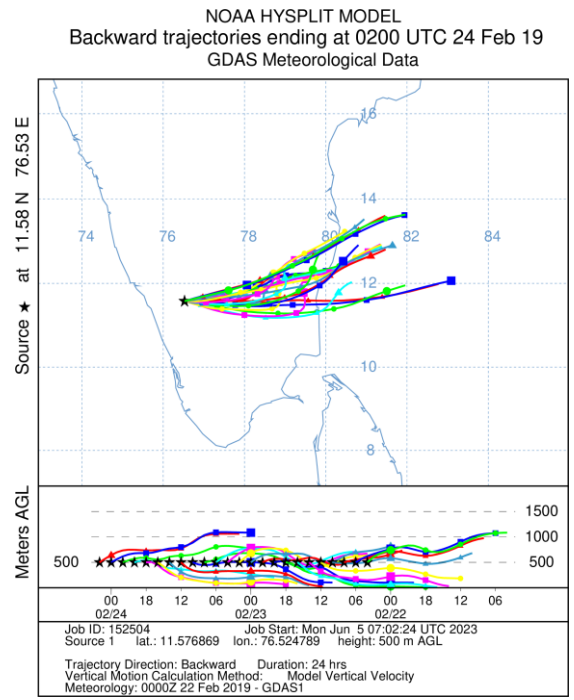

Backward wind trajectory map of Ombetta from 22-28 February, 2019, 500m above seal level. The top pictures show the magnified image of the trajectories.

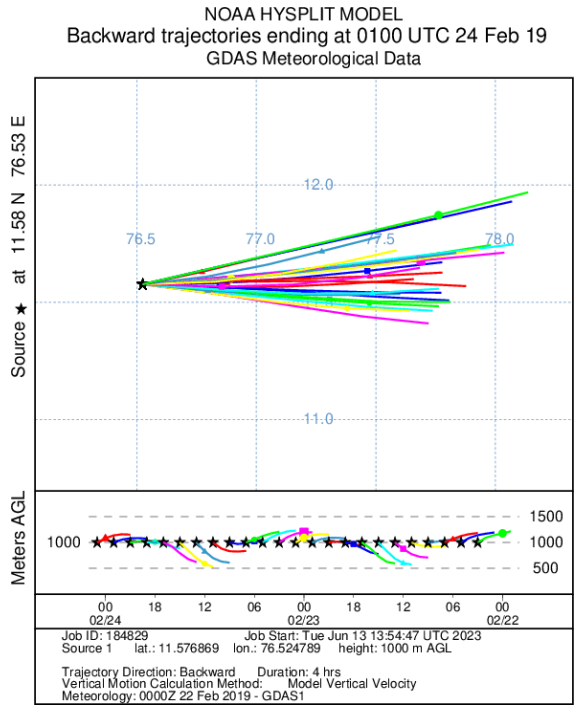

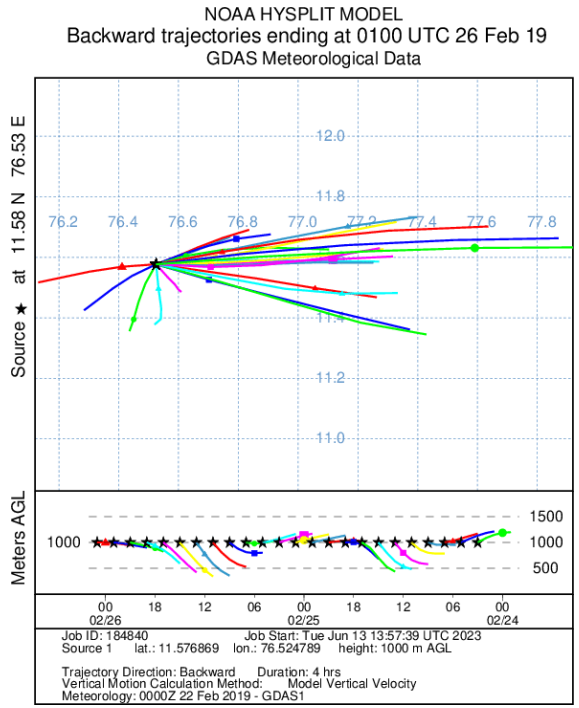

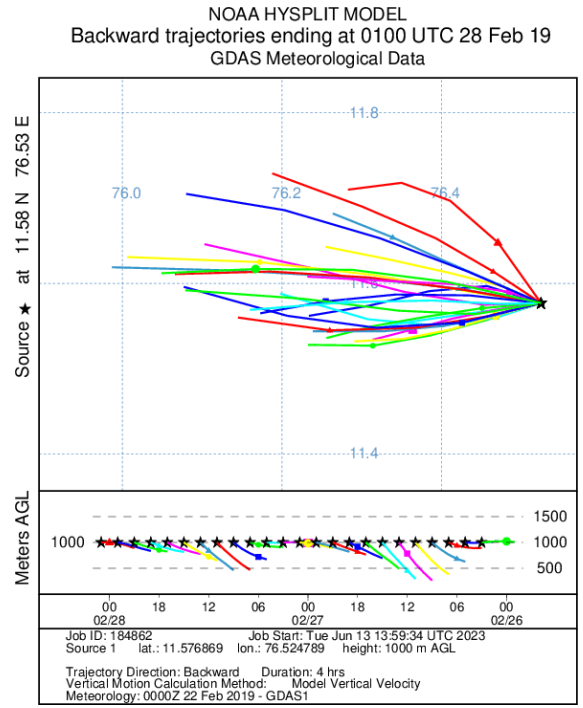

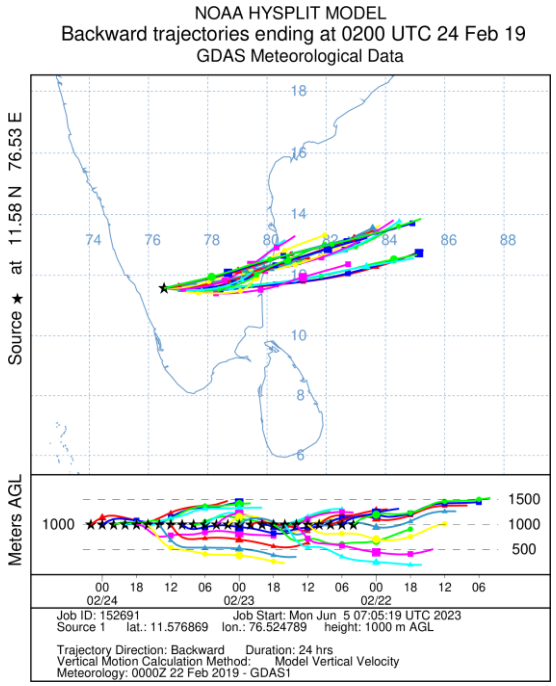

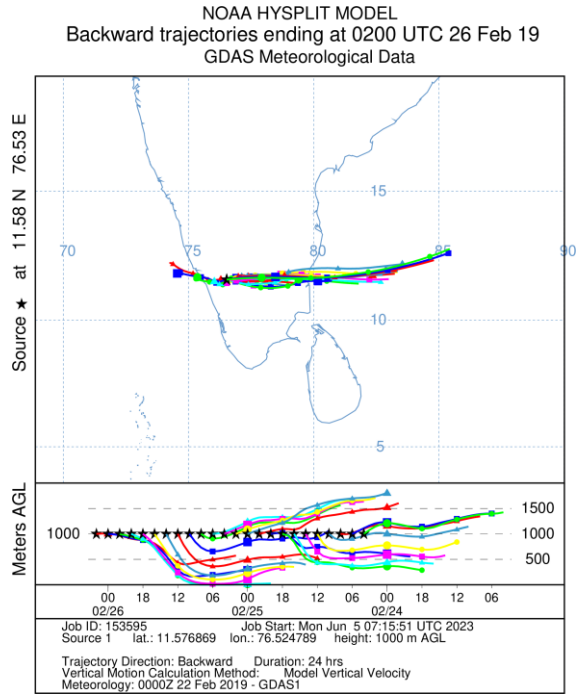

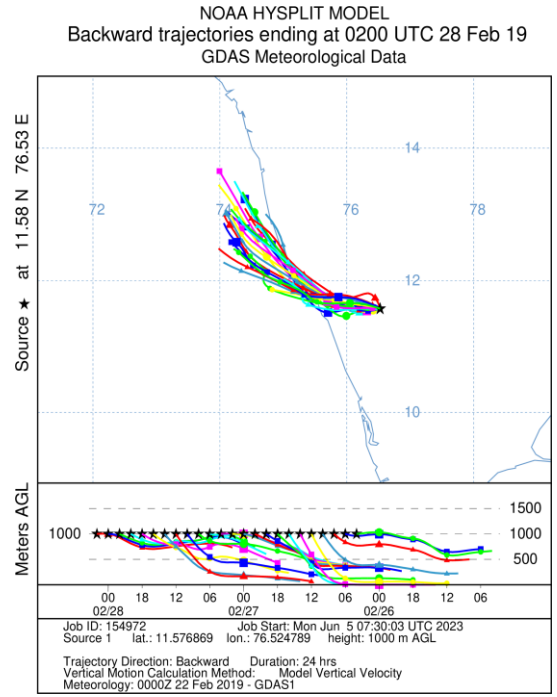

Backward wind trajectory map of Ombetta from 22-28 February, 2019, 1000m above seal level. The top pictures show the magnified image of the trajectories.

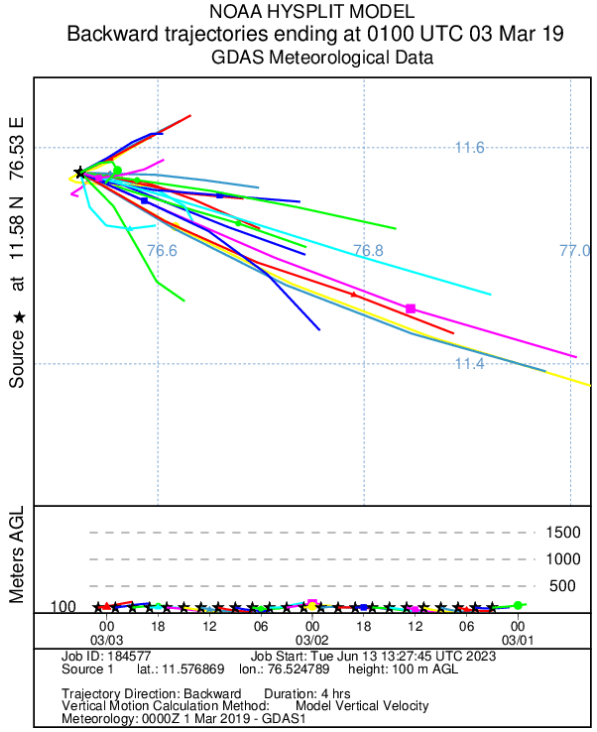

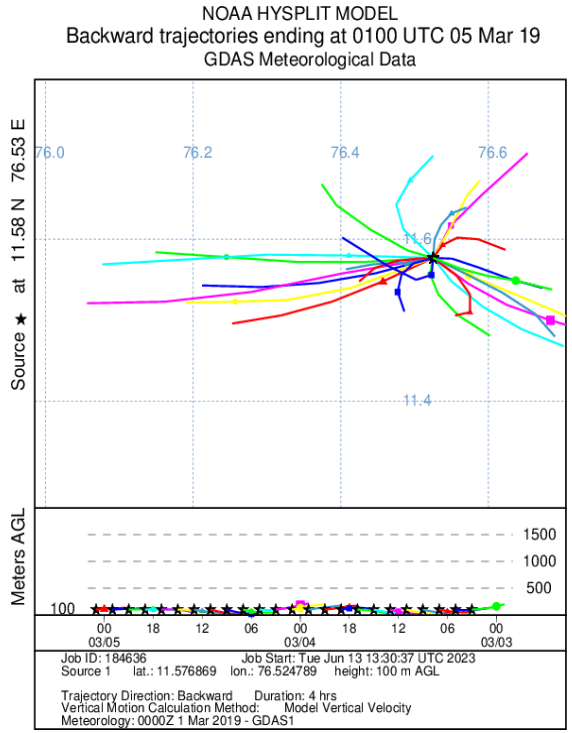

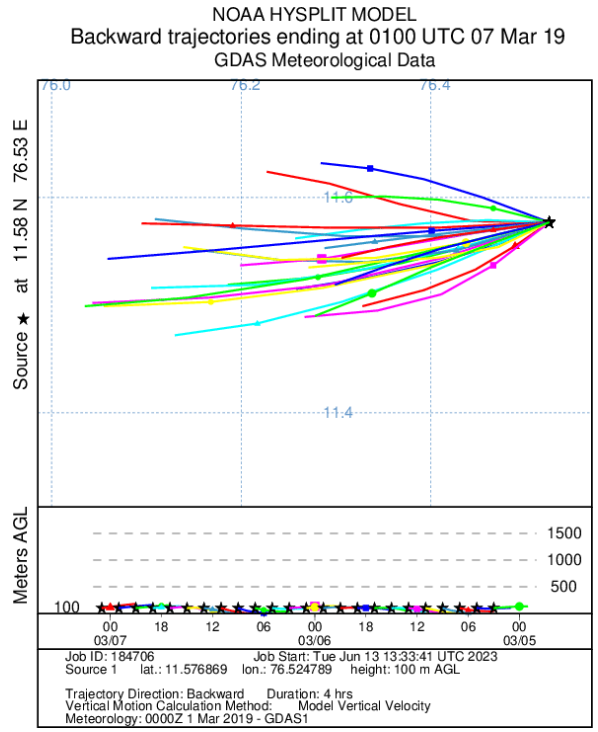

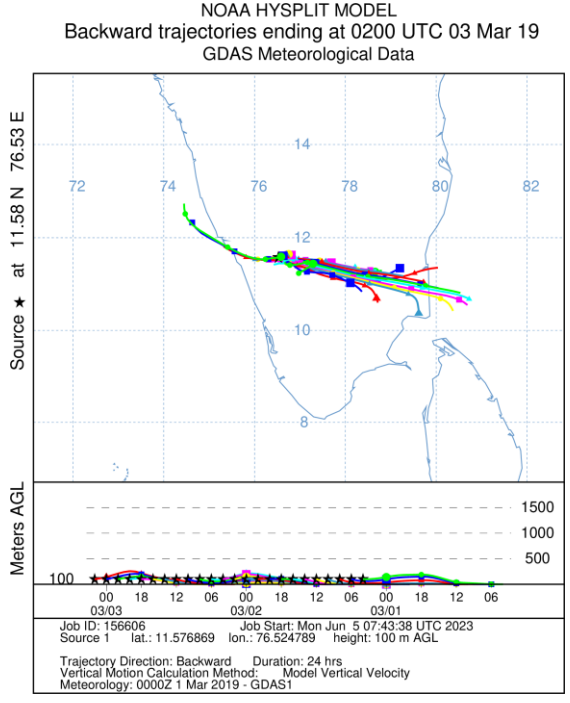

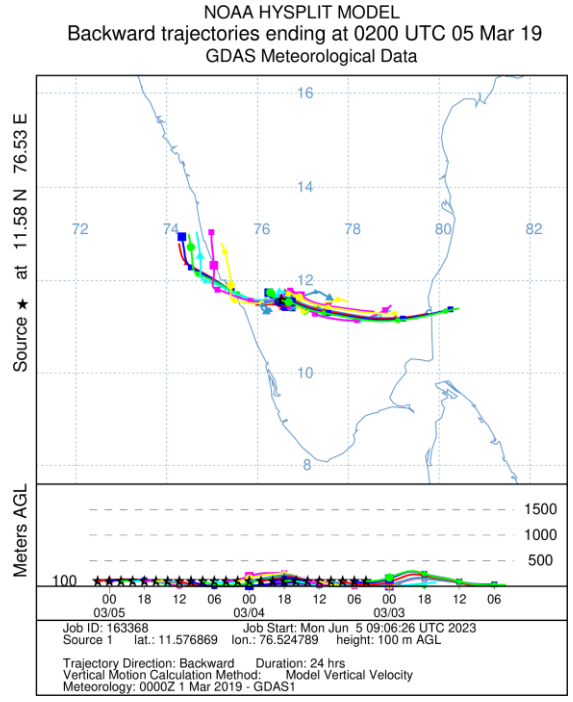

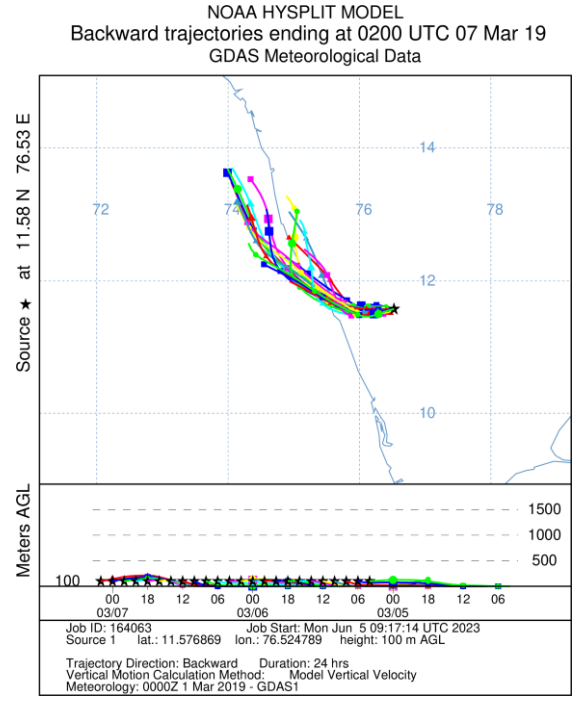

Backward wind trajectory map of Ombetta from 01-07 March, 2019, 100m above seal level. The top pictures show the magnified image of the trajectories.

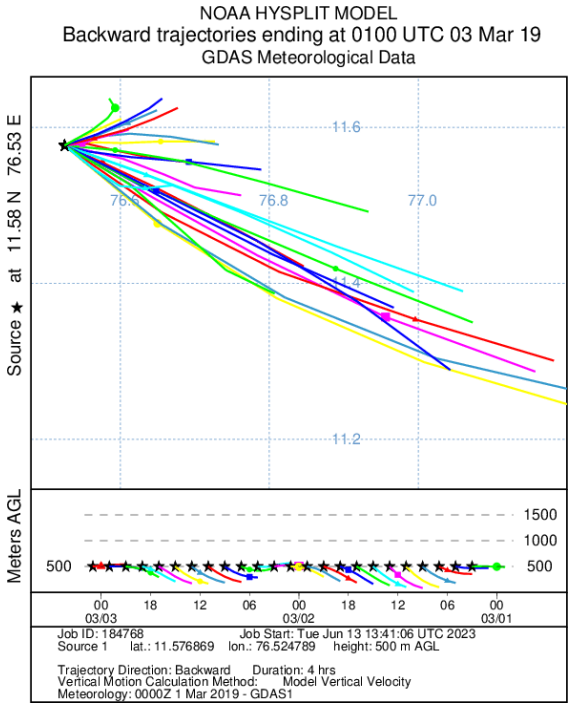

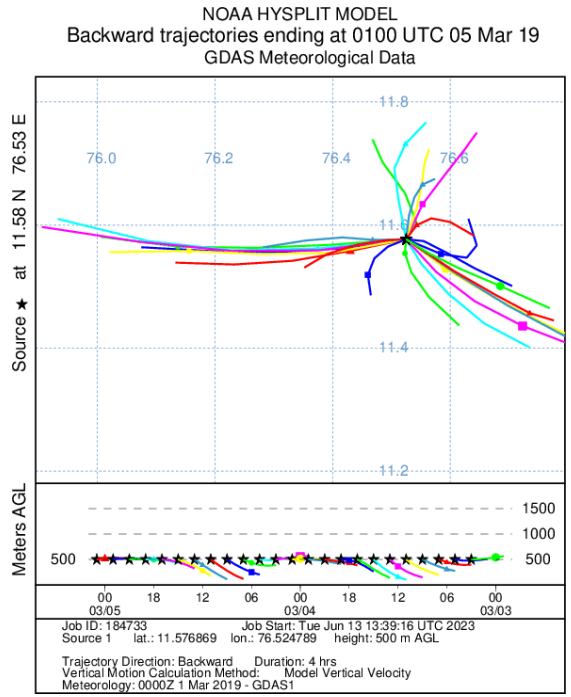

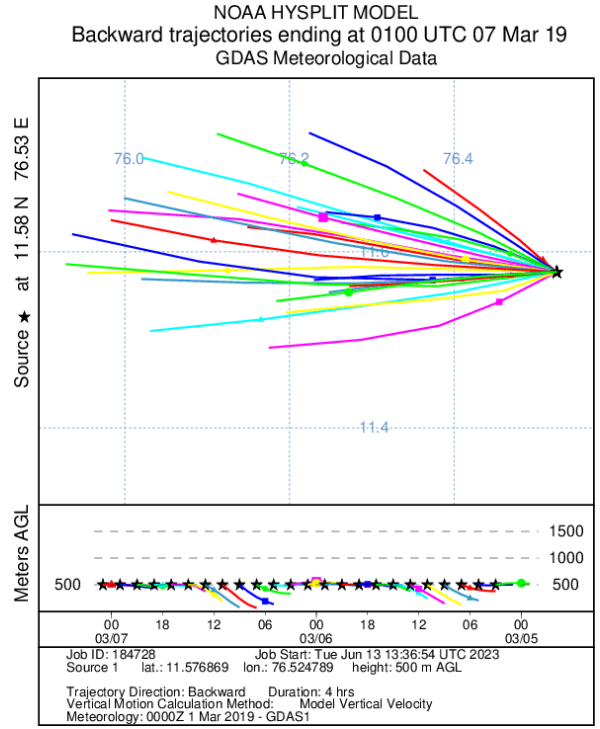

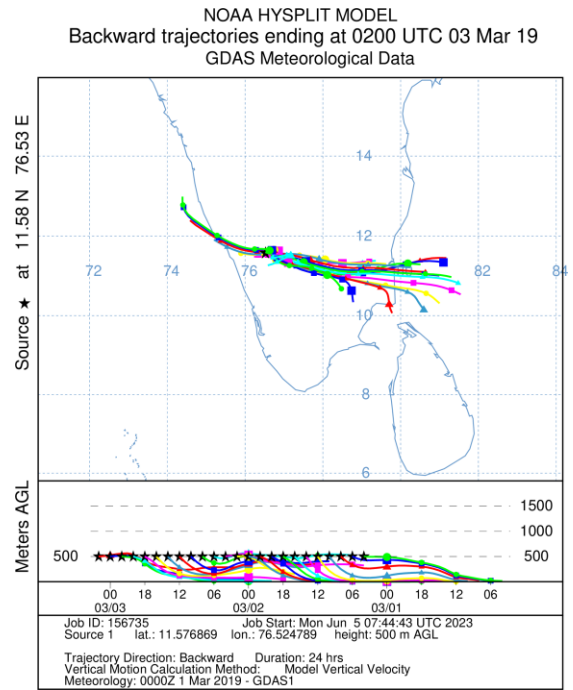

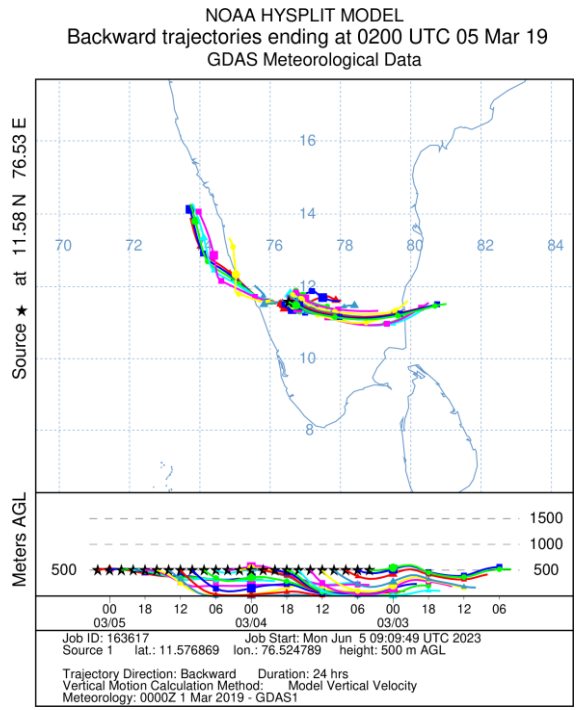

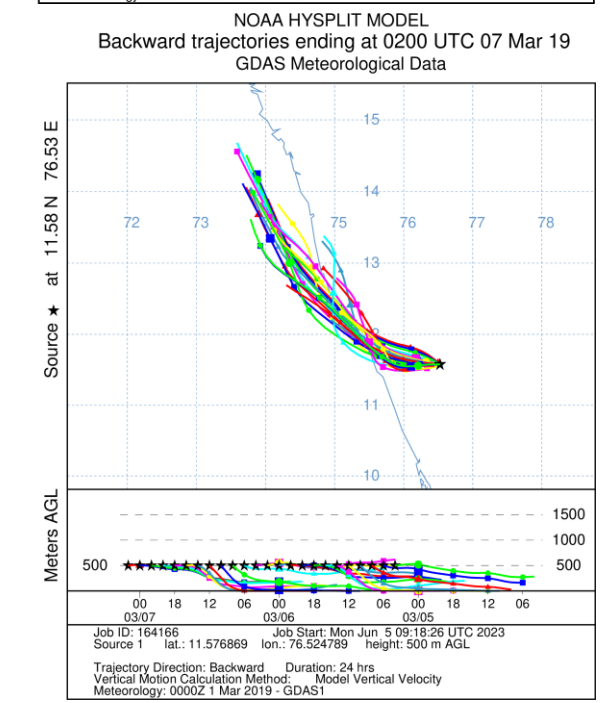

Backward wind trajectory map of Ombetta from 01-07 March, 2019, 500m above seal level. The top pictures show the magnified image of the trajectories.

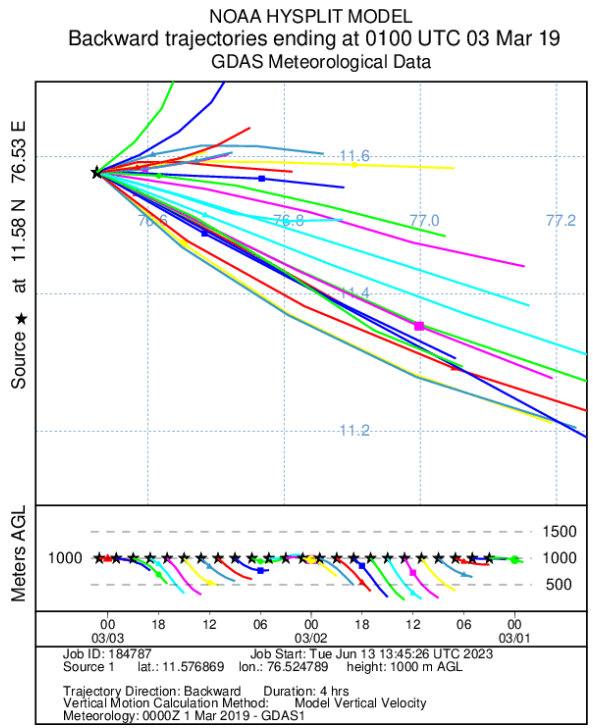

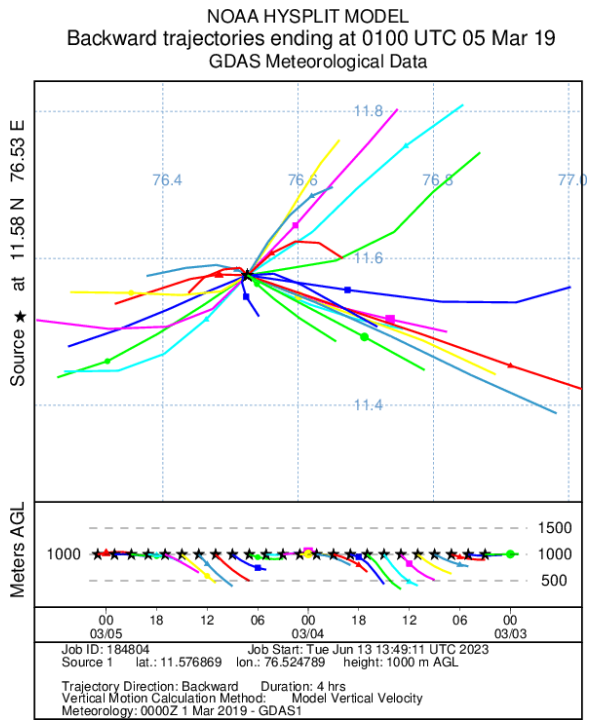

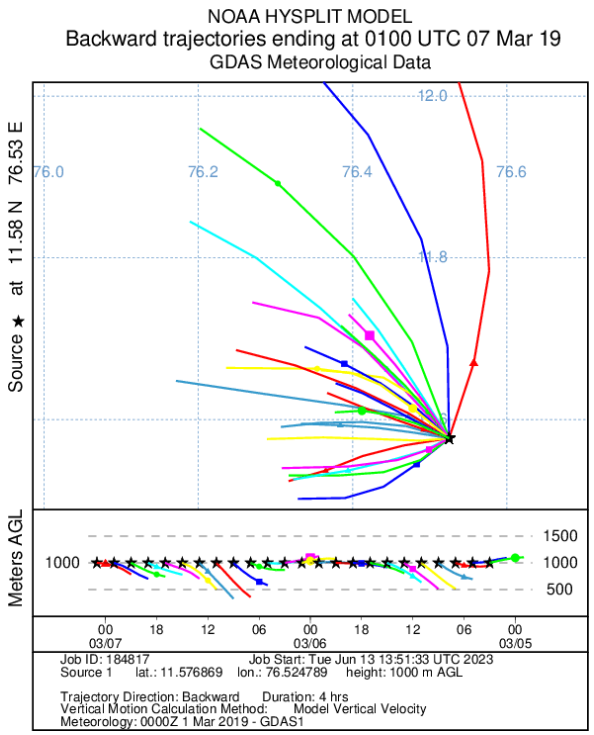

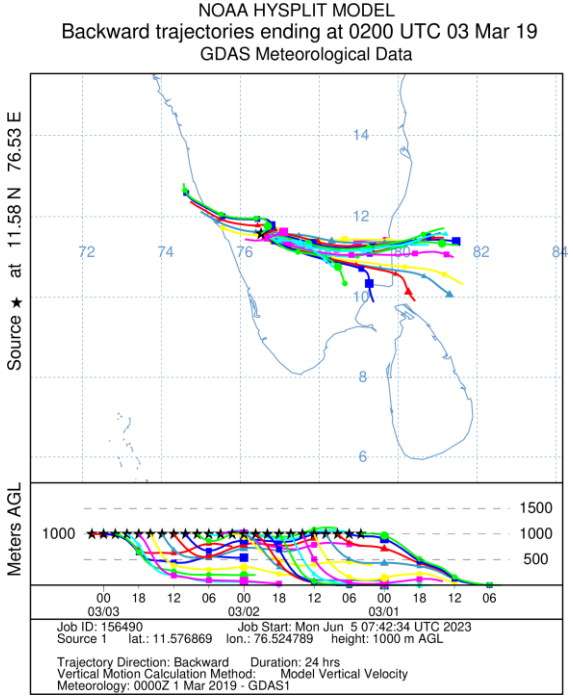

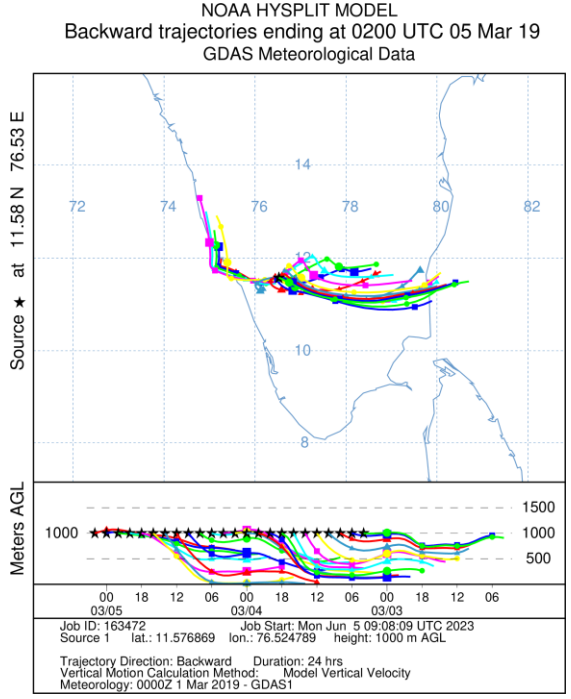

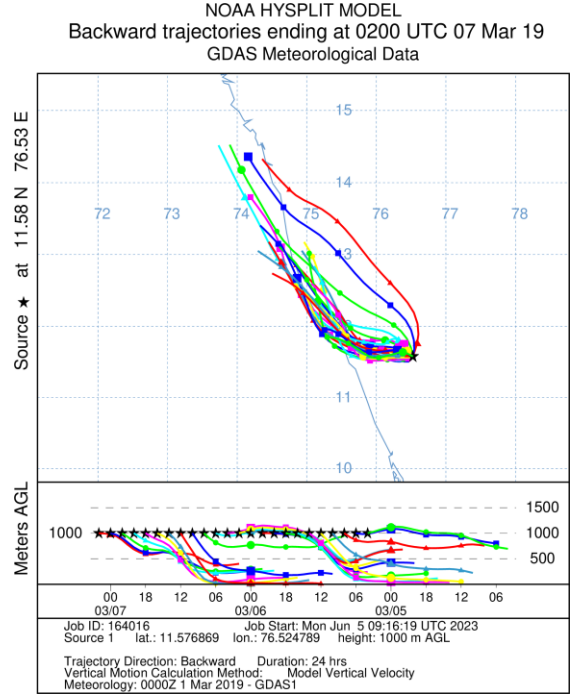

Backward wind trajectory map of Ombetta from 01-07 March, 2019, 1000m above seal level. The top pictures show the magnified image of the trajectories.

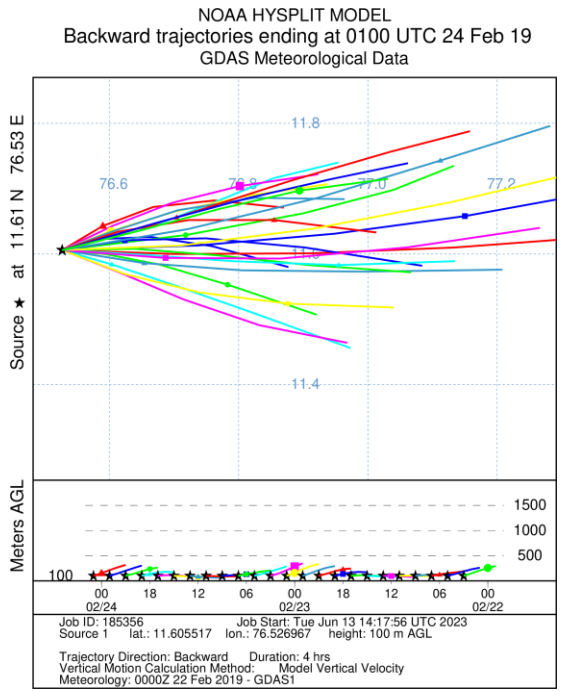

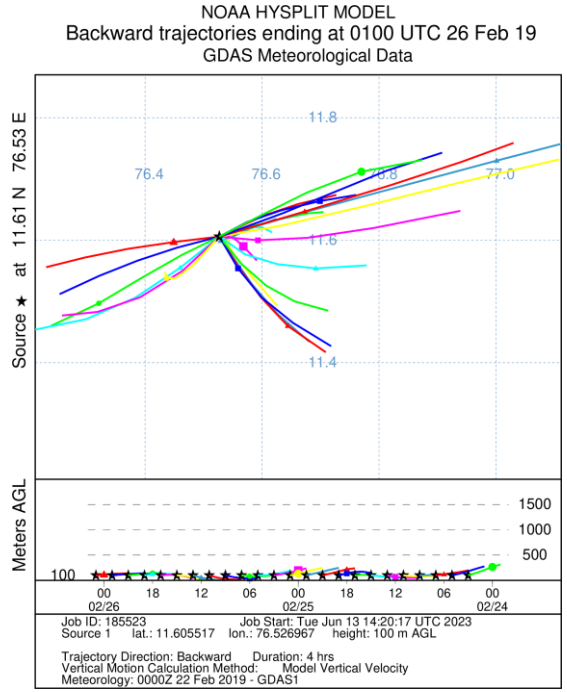

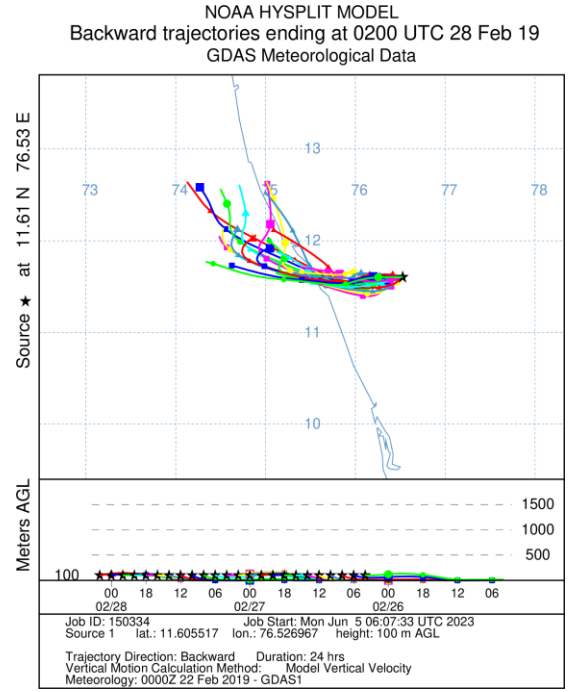

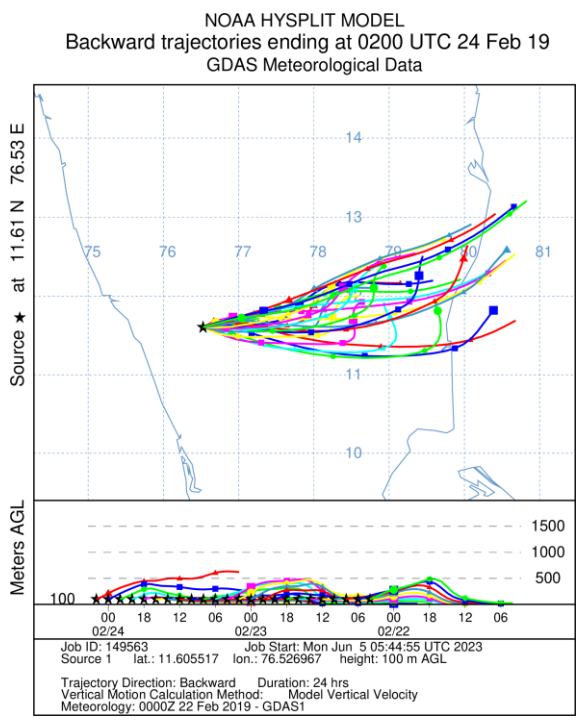

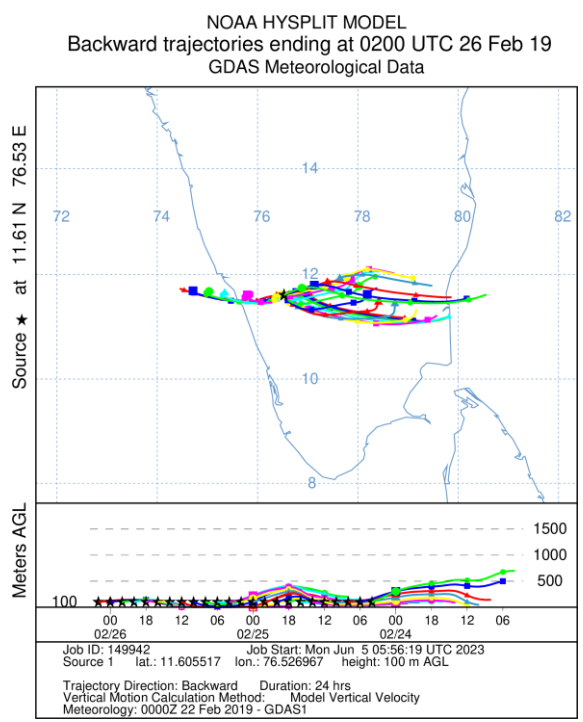

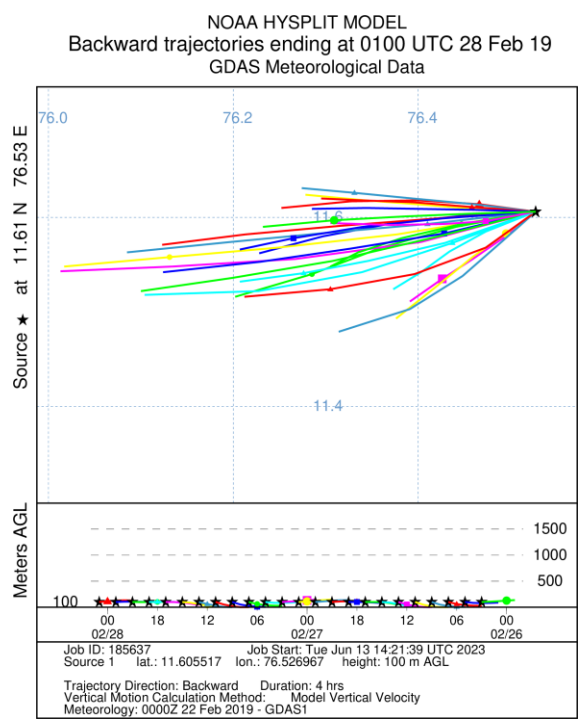

Backward wind trajectory map of Imbrella from 22-28 February, 2019, 100m above seal level. The top pictures show the magnified image of the trajectories.

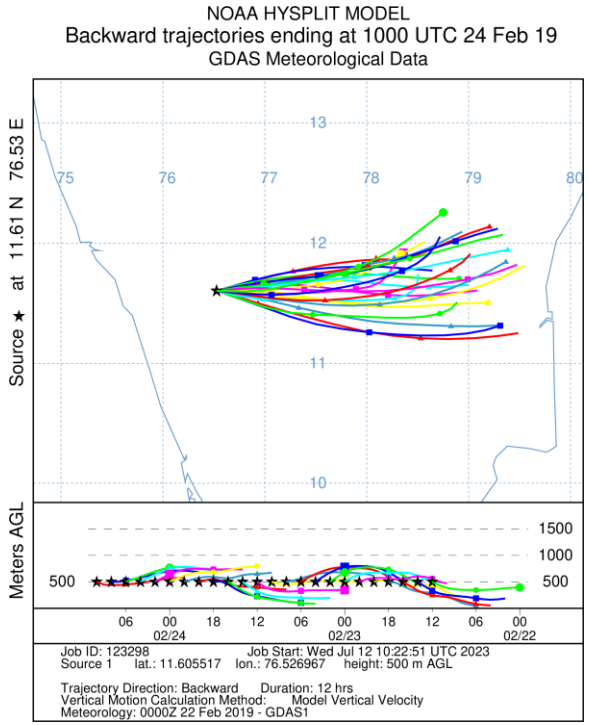

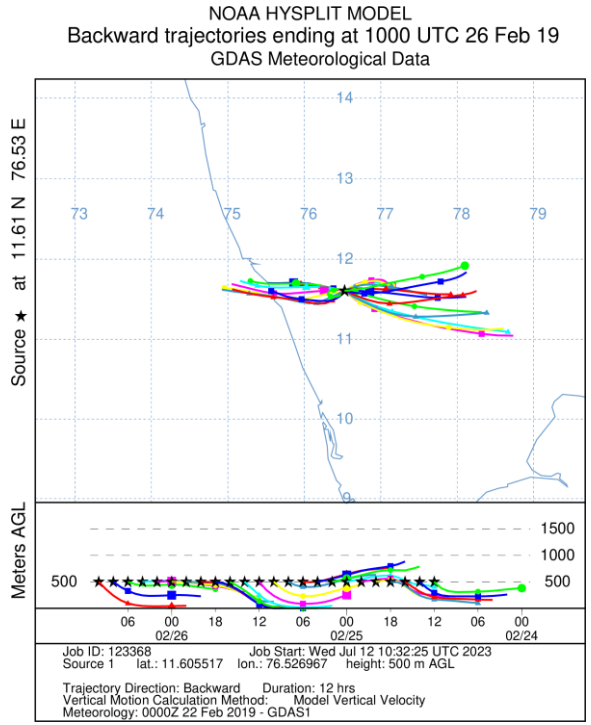

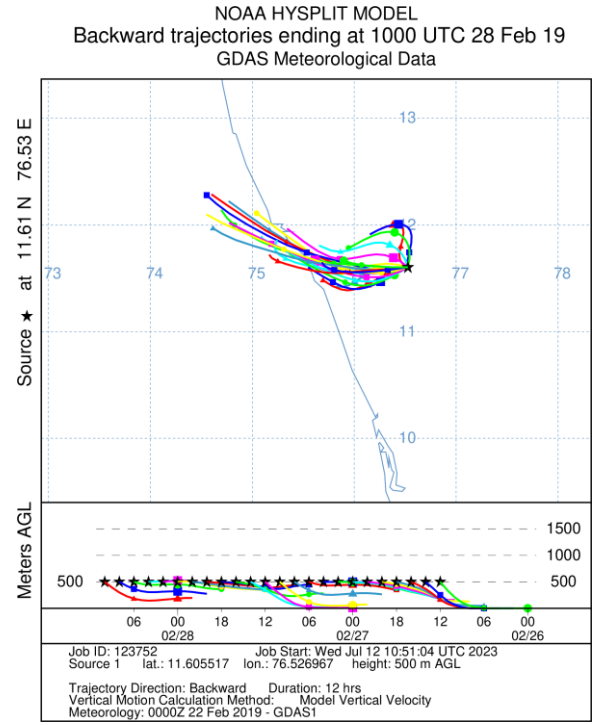

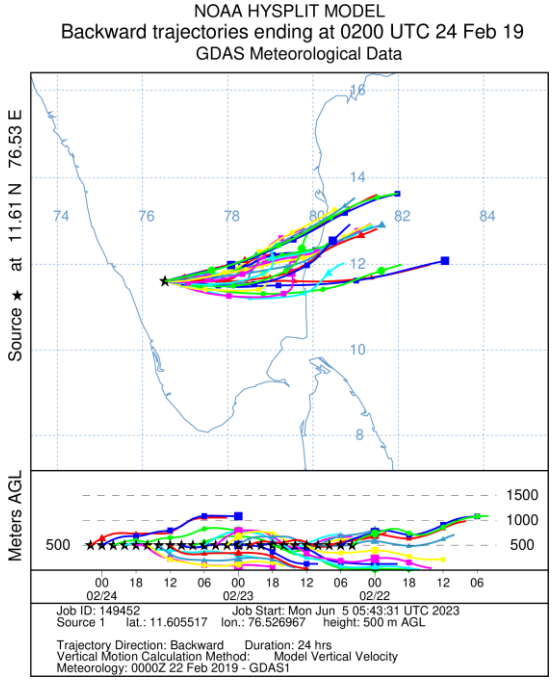

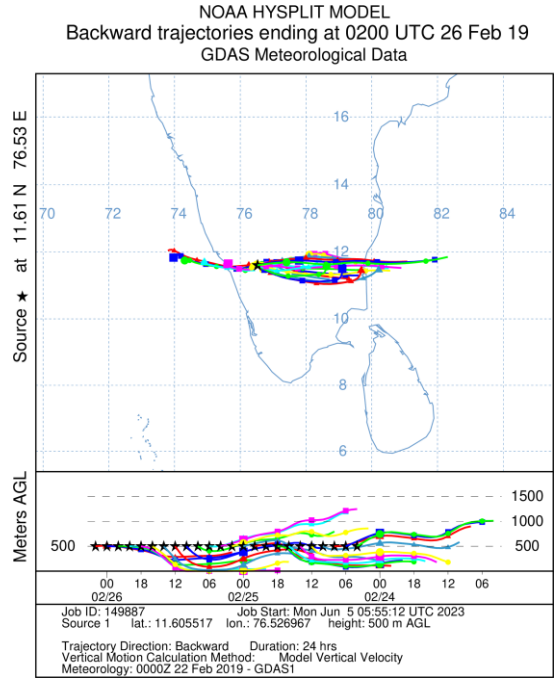

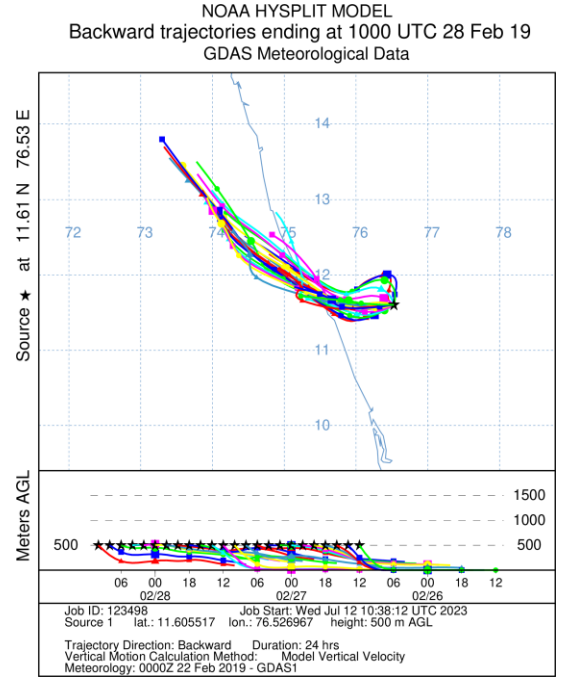

Backward wind trajectory map of Imbrella from 22-28 February, 2019, 500m above seal level. The top pictures show the magnified image of the trajectories.

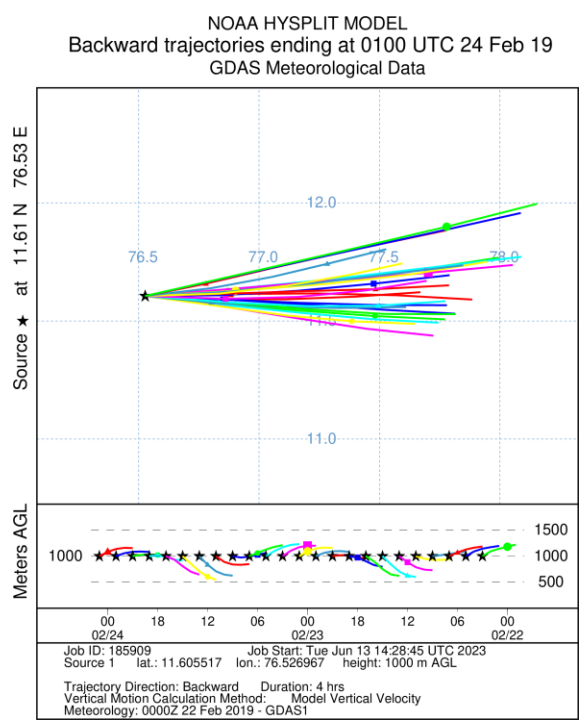

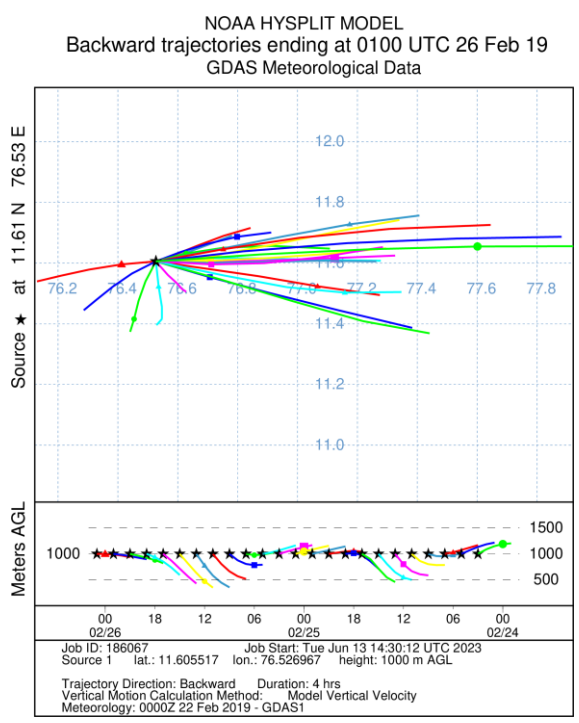

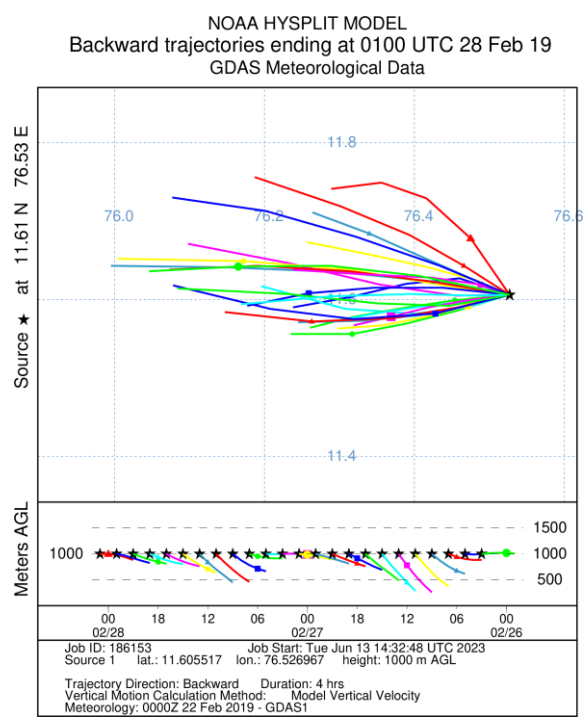

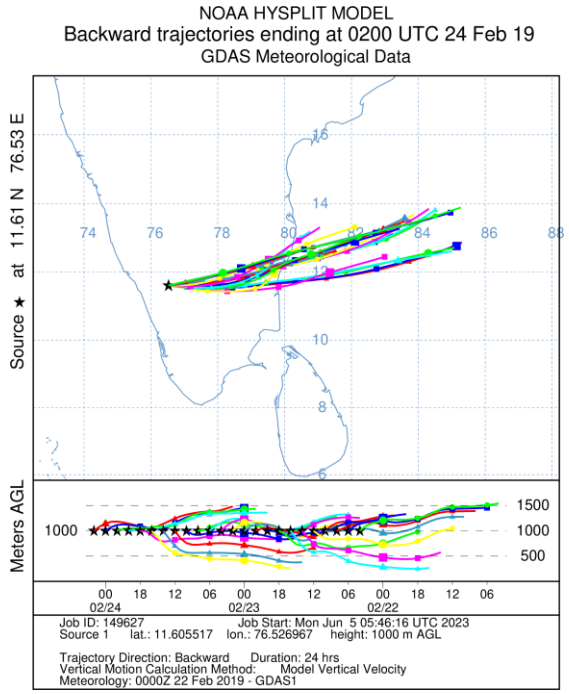

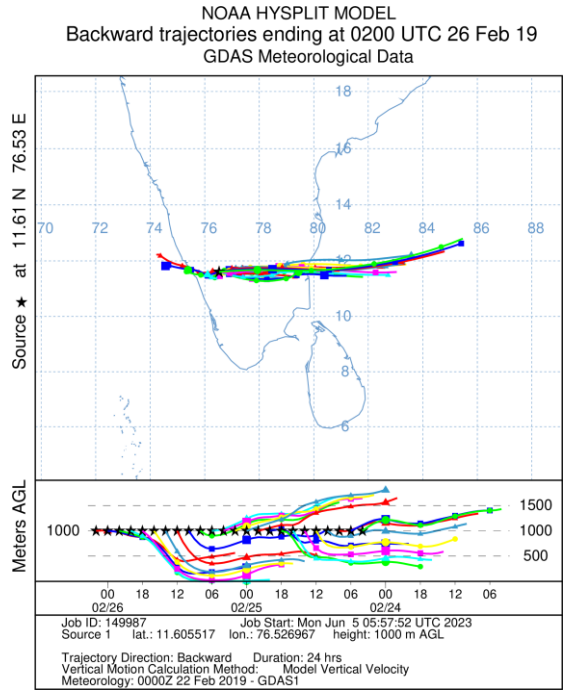

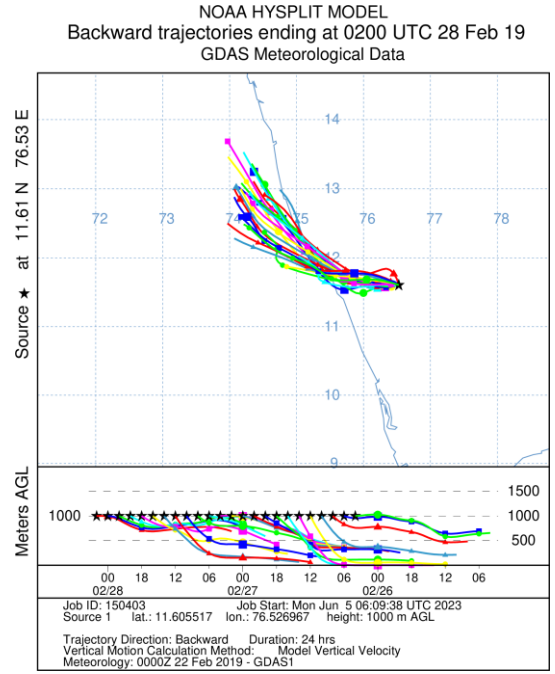

Backward wind trajectory map of Imbrella from 22-28 February, 2019, 1000m above seal level. The top pictures show the magnified image of the trajectories.

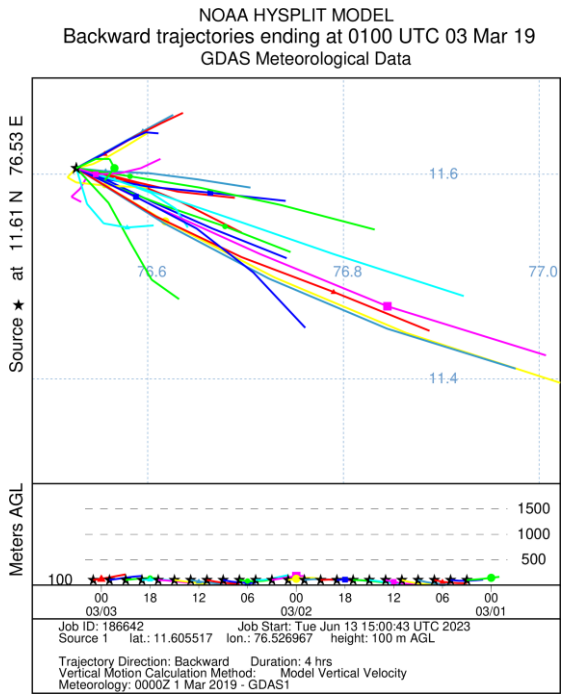

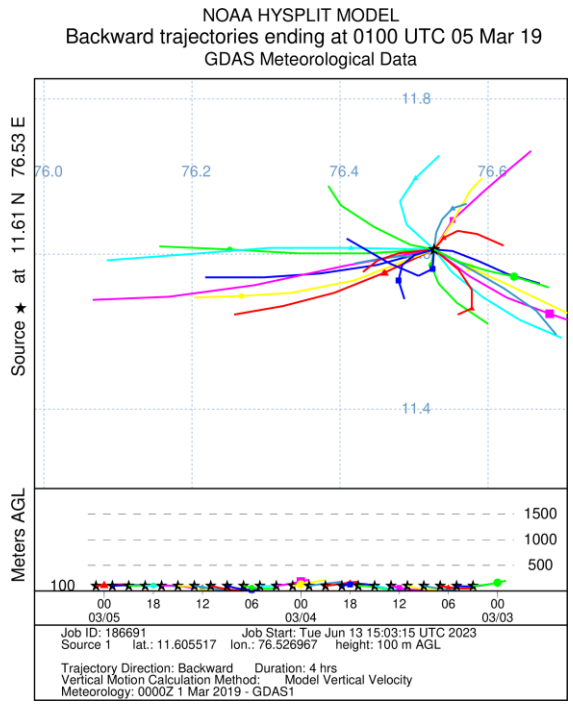

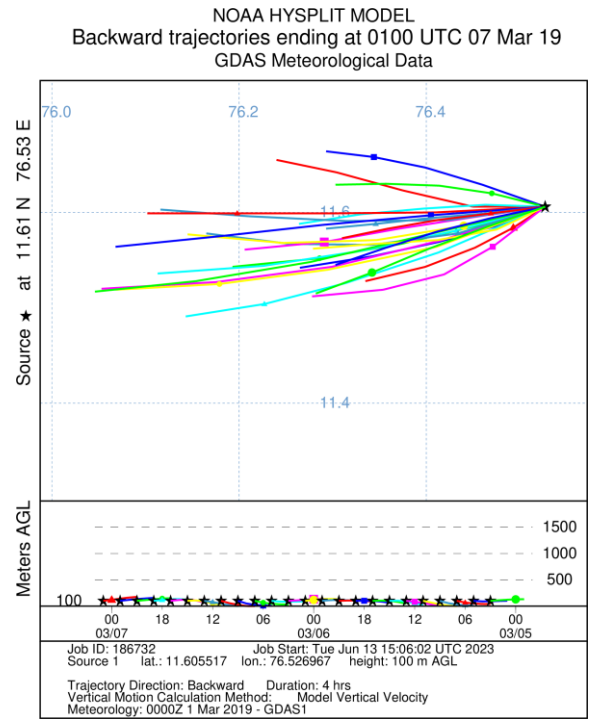

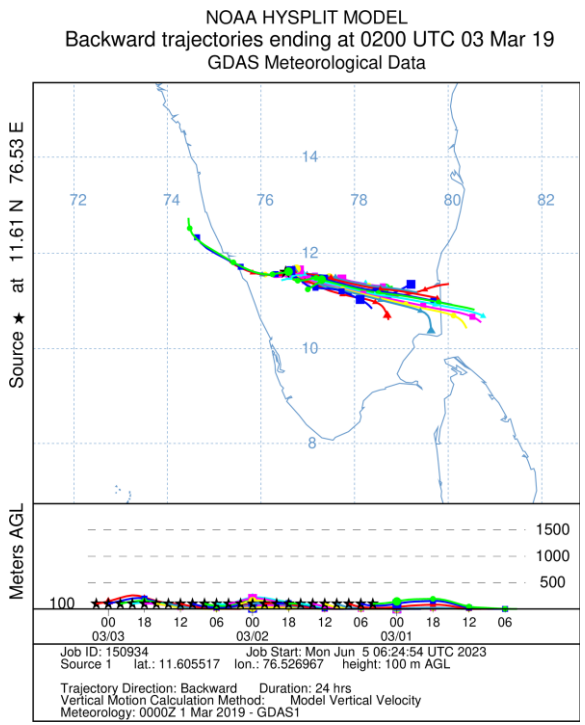

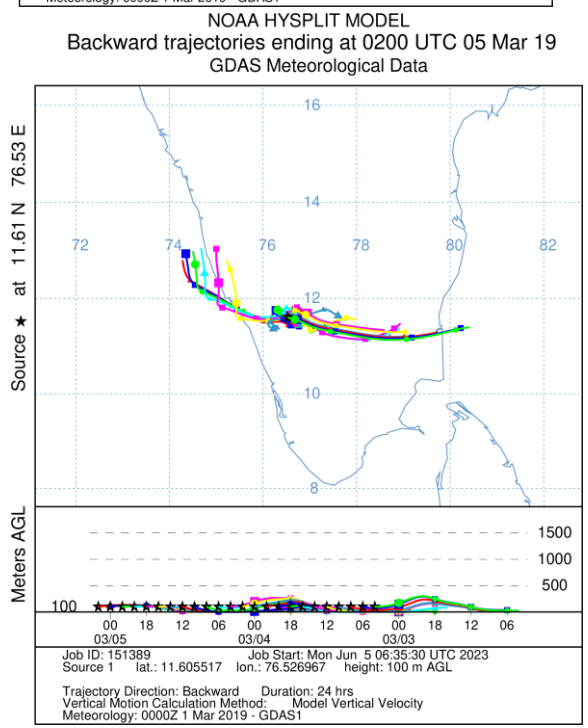

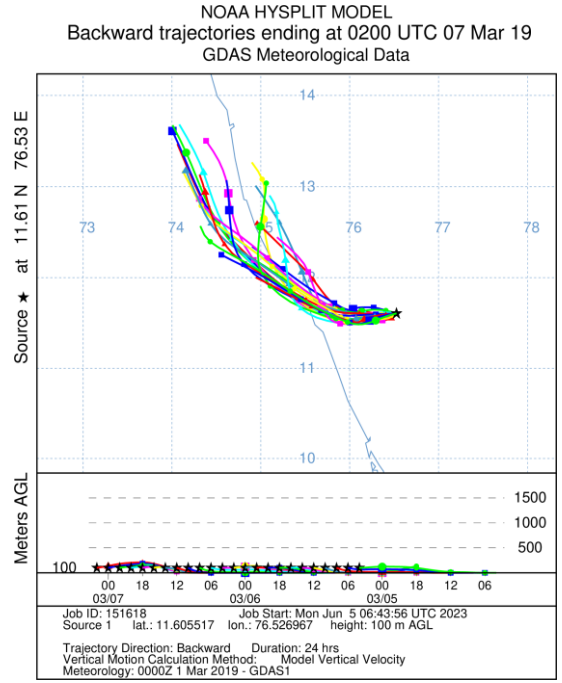

Backward wind trajectory map of Imbrella from 01-07 March, 2019, 100m above seal level. The top pictures show the magnified image of the trajectories.

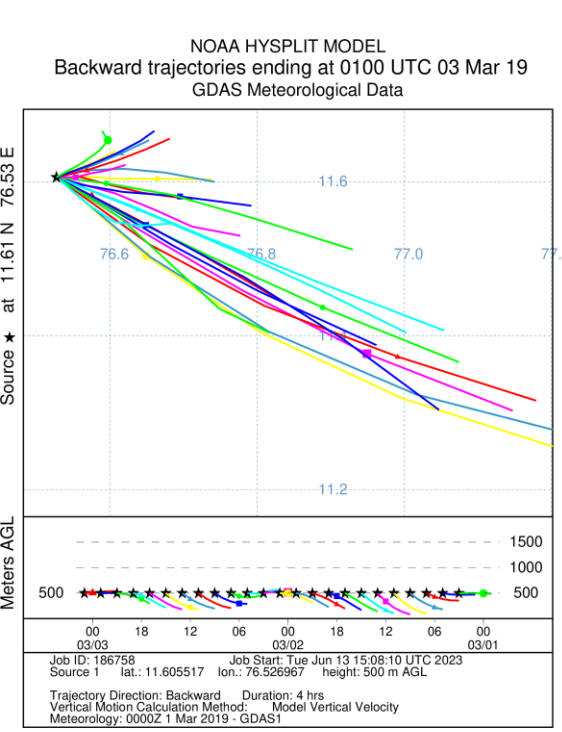

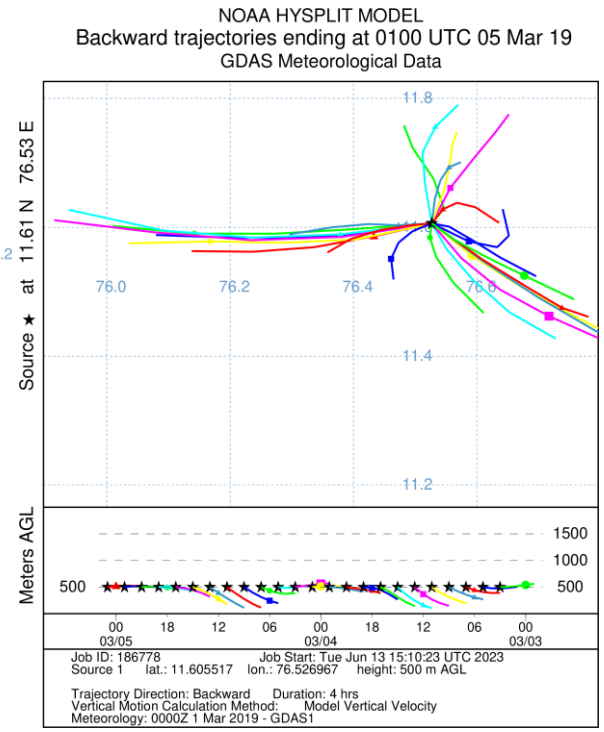

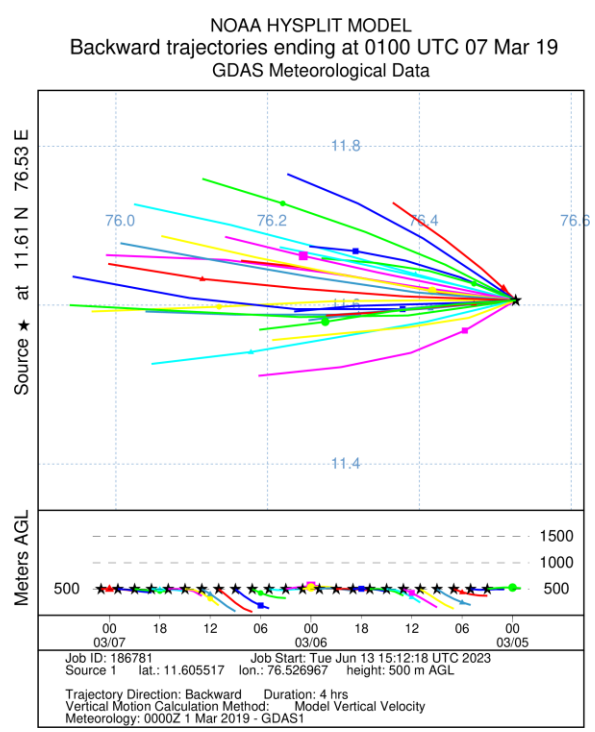

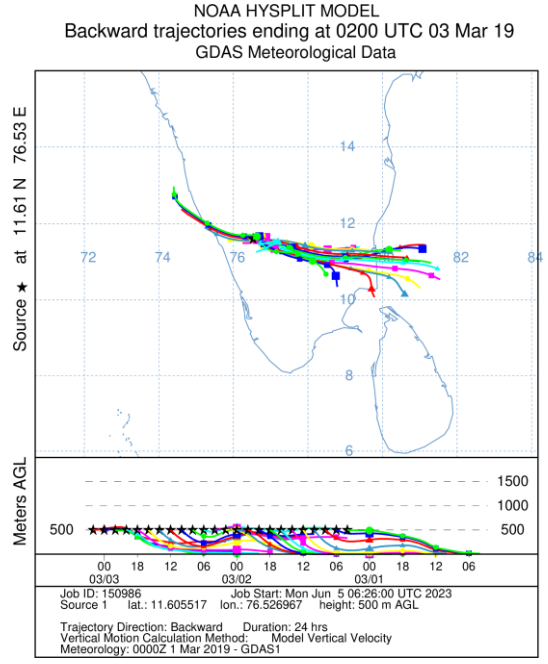

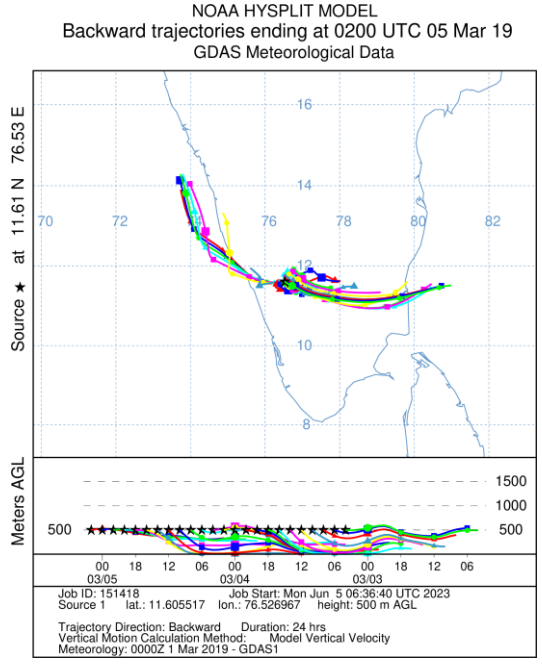

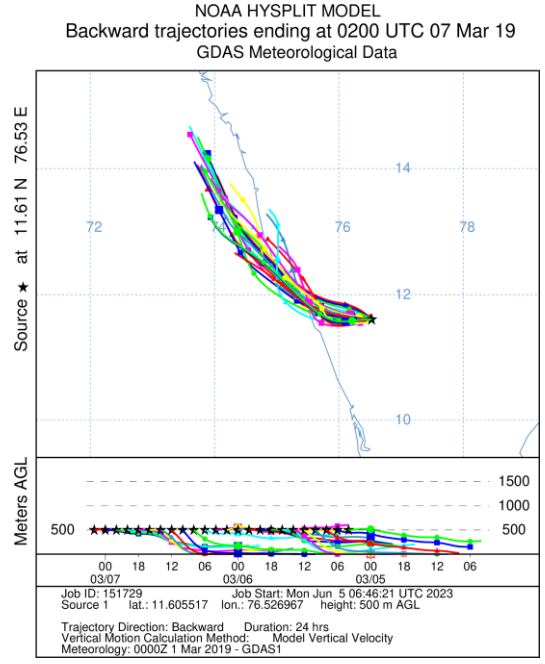

Backward wind trajectory map of Imbrella from 01-07 March, 2019, 500m above seal level. The top pictures show the magnified image of the trajectories.

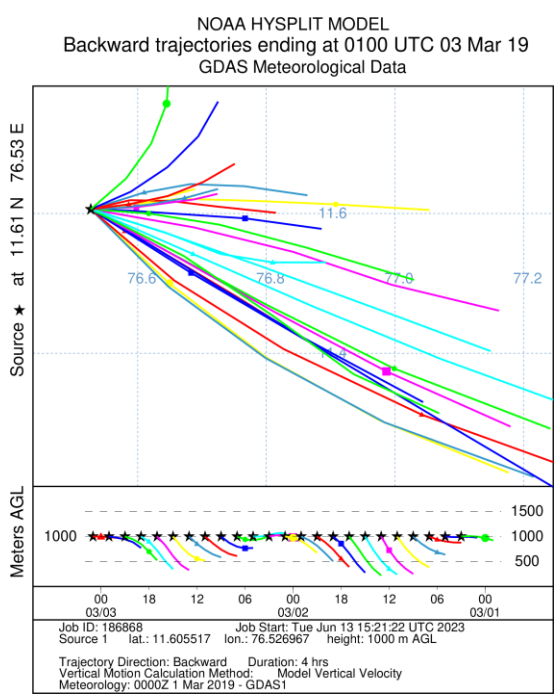

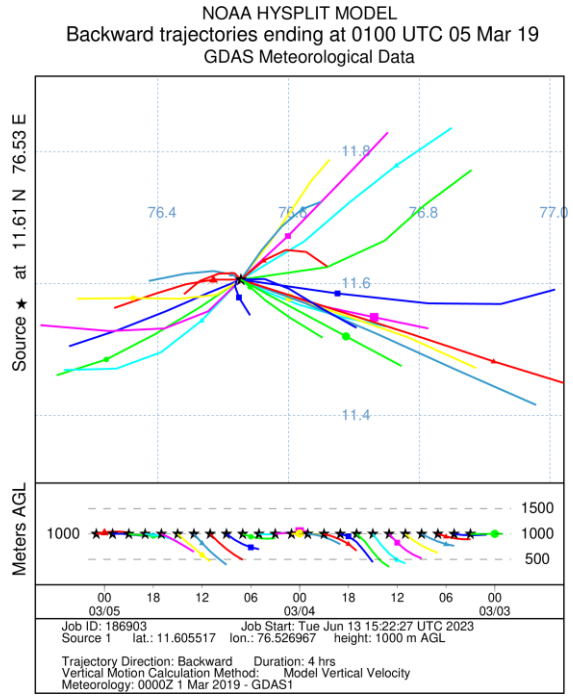

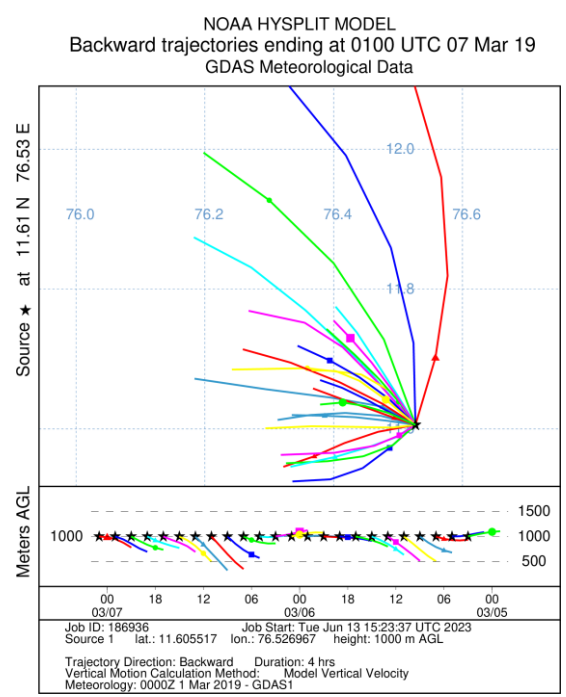

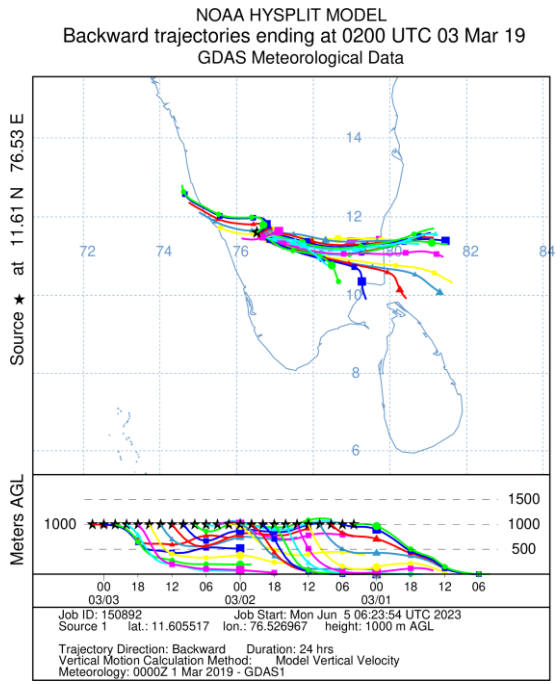

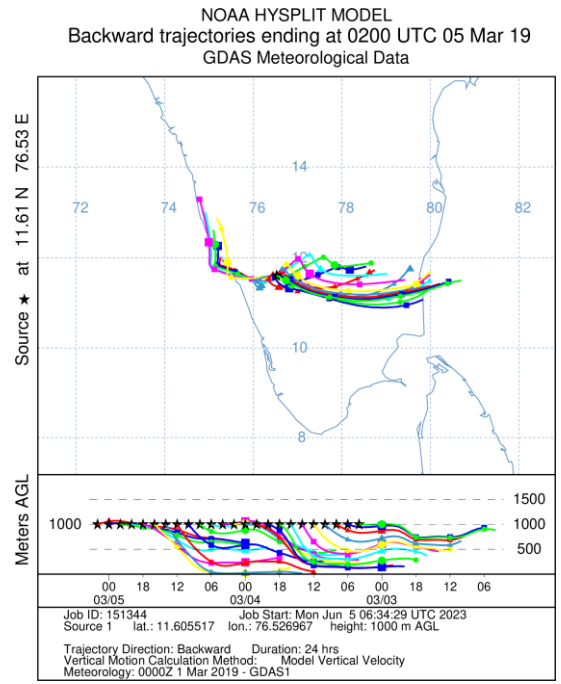

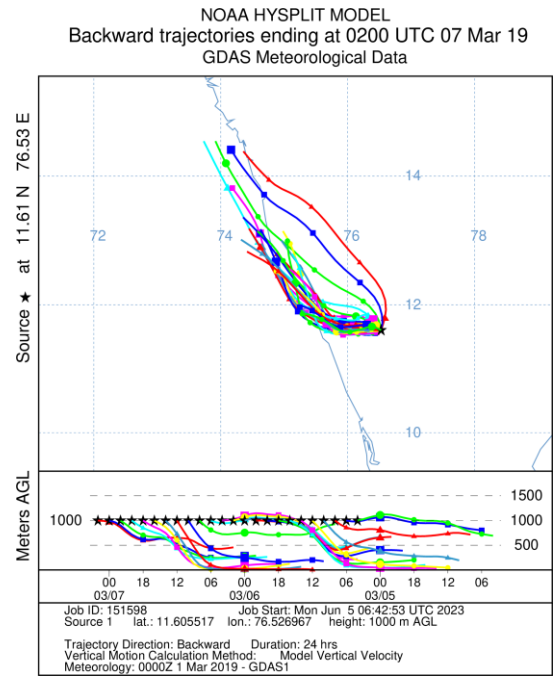

Backward wind trajectory map of Imbrella from 01-07 March, 2019, 1000 m above seal level. The top pictures show the magnified image of the trajectories.